CSA GROUP™

STANDARDS RESEARCH

Development of a Geotechnical Design Standard for Buildings in Canada

February 2022

Authors

Gordon A. Fenton, **P.Eng., Ph.D., FEIC, FCAE,** Dalhousie University

Pengpeng He, **Ph.D.,** Dalhousie University

Gennaro Esposito, **P.Eng., Ph.D. Candidate,** Dalhousie University

Reza Rahimi, **EIT, Ph.D.,** Dalhousie University

Project Advisory Panel

Paul Wilson, **P.Eng., M.Sc., P.Geo.,** Thurber Engineering Ltd., Vancouver

Dennis Becker, **P.Eng., Ph.D.,** Golder/WSP, Calgary

Jennifer Teague, **Ph.D.,** CSA Group

Mark Braiter, **MBA,** CSA Group (Project Lead)

Financial Support

The work is supported in part by Mitacs (Grant No.: IT21047) and the Natural Sciences and Engineering Research Council of Canada.

Table of Contents

Executive Summary

Canadians are in the enviable position of having created a world-leading reliability-based geotechnical design code for bridges, namely Section 6 Foundations and Geotechnical Systems of CSA S6:19, *Canadian highway bridge design code* (CHBDC). Further research is now required to develop similar design provisions for the buildings, where a minimum geotechnical standard is currently lacking in Canada. It is anticipated that such design provisions would be beneficial and could be considered for a future standard.

This research summarizes the findings of a study that investigated target reliability levels for geotechnical systems and the resulting resistance factors required to achieve these reliability targets within a load and resistance factor design (LRFD) framework. The geotechnical problems considered include:

- Seismic design of deep foundations;
- Seismic and wind loading design of shallow foundations;
- Sliding resistance of shallow foundations; and
- Sliding and overturning resistance of retaining walls.

This research also summarizes the results of an investigation into direct reliability-based design as an alternative to the LRFD approach.

While most of the unknown resistance factors needed to develop a geotechnical design standard for buildings in Canada are calibrated in this research, areas that require additional research for the calibration of geotechnical resistance factors are identified in the summary.

"It is becoming increasingly apparent to the geotechnical community that the lack of a minimum standard of practice for a critical component of each building, its foundation, may lead to either inefficient designs or to designs that fall below a societally acceptable level of safety."

1 Introduction

The National Building Code of Canada (NBC) [1] lacks a legally enforceable minimum standard for geotechnical design. It is becoming increasingly apparent to the geotechnical community that the lack of a minimum standard of practice for a critical component of each building, its foundation, may lead to either inefficient designs or to designs that fall below a societally acceptable level of safety. At the moment, building foundations in Canada are largely designed using manuals, such as the Canadian Foundation Engineering Manual (CFEM) [2], or codes of practice from other jurisdictions, such as the *Eurocode 7: Geotechnical design* (EN 1997) [3], so there is no enforceable minimum safety standard for building foundations.

To develop a minimum safety standard for the design of foundations and geotechnical systems of buildings for Canada, the following issues need to be addressed:

1. Determine acceptable target lifetime reliability levels for geotechnical systems. That is, how should these compare to lifetime reliability targets for structural systems? Should they be the same or higher when cost of repair is taken into account? How should failure consequence level be accounted for in these target reliabilities?
2. Determine the resistance factors required to achieve the acceptable target lifetime reliability levels determined in Eq. (1) for various geotechnical problems and limit states, and for a range of uncertainty levels in the ground resistance and in the applied load.
3. Resistance factors required for the seismic design of foundations and geotechnical systems are essentially unknown. Research into what these seismic design factors should be is needed.

The design of civil engineering systems employs an approach broadly known as limit state design (LSD), a framework in which various possible limit states are designed using a methodology called load and resistance factor design (LRFD). In Canada, the basic idea is to produce a design that satisfies an inequality of the following form for each limit state:

$$\phi_g \hat{R} \geq \sum \alpha_i \hat{F}_i, \qquad (1)$$

where ϕ_g is the geotechnical resistance factor at the limit state being considered, $\hat{R}$ is the characteristic geotechnical resistance at the same limit state, $\hat{F}_i$ is the i^{th} characteristic load, and α_i is the load factor corresponding to $\hat{F}_i$. Usually, designs are aimed to satisfy Eq. (1) at, or close to, the equality to avoid over-conservatism.

The usual approach to calibration of the load and resistance factors appearing in Eq. (1) is to first calibrate the load factor, α_i, which is generally selected so that the factored load, $\alpha_i \hat{F}_i$, has a suitably small probability of exceedance over the design life of the system. There have been many studies on the calibration of load factors, as reflected in the literature. In Canada, the pioneering research by Allen [4] and the calibration by Bartlett et al. [5] for the 2005 edition of the NBC [1] provided the basis for the current NBC. Becker [6], [7] provided an excellent state-of-the-art analysis of LRFD for geotechnical design in Canada.

The LRFD approach utilizes a geotechnical resistance factor, typically less than 1, to scale the geotechnical resistance to values small enough to achieve the target safety level or the target maximum acceptable failure probability. The target failure probability depends on potential losses, personal and societal safety requirements, and so on — that is, it depends on the consequences of failure. At the time of writing, the geotechnical resistance factors used for buildings in Canada are as specified by the CFEM [2] and as shown in the Structural Commentaries of the NBC User's Guide [8]. Both of these documents are intended as guidance and are not legally binding.

The calibration of the geotechnical resistance factor is somewhat more complicated than the calibration of the load factors. Load factors are purely concerned with the variability of the loads and, as mentioned above, are derived to yield factored loads having a small probability of exceedance over the design lifetime. Once the load factors are known, calibration of the resistance factor involves the following steps, assuming a Monte Carlo simulation-based approach (while an experimental-based approach would be preferable, the cost of setting up, loading, and monitoring the response of many thousands of geotechnical designs on real ground would be astronomical):

1. Select an initial geotechnical resistance factor for use in the design phase.
2. Simulate a series of $i = 1,\ 2,\ \ldots,\ n_{sim}$ random loading conditions and soil property fields according to their various appropriate distributions.
3. Design phase: Replicate the stages of an actual design using characteristic loads, specified load factors, and the appropriate resistance factor, ϕ_g, selected in step 1.
4. Sample the soil at some location (relative to the foundation to be designed) to determine characteristic design soil parameters. In a Monte Carlo simulation approach, this involves sampling the simulated soil parameters (step 2) at some location from the foundation. In an experimental approach to calibration, this involves using the experimentally observed soil parameters.
5. Design the foundation using Eq. (1) for the limit state being considered, the load factors specified by the current code, the resistance factor selected in step 1, and the characteristic soil properties determined in step 4.
6. Using a sophisticated geotechnical model, determine if the designed foundation fails under a randomly simulated load. If so, increment a failure counter, n_{fail}, by 1. In this research, the random finite element method (RFEM) [9], [10] is used to determine whether the designed foundation fails.
7. Repeating from step 2, estimate the failure probability to be $p_f \simeq n_{fail}/n_{sim}$.
8. If the failure probability estimated in step 7 is greater than or less than the maximum acceptable failure probability, the geotechnical resistance factor is reduced or increased and steps 2-5 are repeated until the estimated failure probability is approximately equal to the target maximum acceptable failure probability.

To develop a geotechnical design standard for buildings, the above algorithm can be used to calibrate the geotechnical resistance factors required to achieve maximum acceptable failure probabilities for buildings in Canada for various limit states and geotechnical systems. This research summarizes the results of such a calibration study and is divided into the following topics:

1. Description of the random soil and load models used in this research;
2. Derivation of target reliabilities (maximum acceptable failure probabilities) associated with various limit states and geotechnical systems;
3. Optimization techniques developed for the RFEM;
4. Geotechnical resistance factors required for seismic design of deep foundations;
5. Geotechnical resistance factors required for seismic and wind loading bearing capacity design of shallow foundations;
6. Geotechnical resistance factors required for sliding resistance design of shallow foundations;
7. Geotechnical resistance factors required for sliding and overturning resistance design of gravity retaining walls;

8. Reliability-based design versus LRFD of shallow foundations; and
9. A summary of the results.

2 Random Soil and Load Models

2.1 Random Soil Models

In this research, the soil has several spatially varying random properties that are simulated in the Monte Carlo analyses, including unit weight, undrained shear strength, effective friction angle, and shear wave velocity. These are modelled using either lognormally distributed random fields (unit weight, undrained shear strength, and shear wave velocity) or tanh distributed random fields (effective friction angle, see Ref. [11] for more details on tanh distribution). All soil properties are assumed to be independent for simplicity [12].

A random field is a collection of random variables whose values are associated with each spatial location. For this research, only the undrained shear strength field, s_u, is described for illustration. The other soil properties are treated similarly, albeit with potentially different marginal distributions. The undrained shear strengh is assumed to be lognormally distributed with specified mean, μ_{s_u}, and standard deviation, σ_{s_u}. Because the undrained shear strength is assumed to be lognormally distributed, its logarithm, lns_u, is normally distributed with parameters,

$$\sigma^2_{\ln s_u} = \ln\left(1 + v^2_{s_u}\right), \tag{2a}$$

$$\mu_{\ln s_u} = \ln\left(\mu_{s_u}\right) - \frac{1}{2}\sigma^2_{\ln s_u}, \tag{2b}$$

where ν_{s_u} is the coefficient of variation of s_u. Simulation of undrained shear strength values then proceeds by first simulating a sequence of normally distributed random variables, G, and then transforming to undrained shear strength according to

$$s_u = \exp\left\{\mu_{\ln s_u} + \sigma_{\ln s_u} G\right\}. \tag{3}$$

Values within each random field are correlated with one another as a function of the distance between them. This research uses an isotropic exponentially decaying Markov correlation function, defined by

$$\rho(\tau_{ij}) = \exp\left\{\frac{-2\tau_{ij}}{\theta}\right\}, \tag{4}$$

where $\tau_{ij}=|\underset{\sim}{x}_i - \underset{\sim}{x}_j|$ is the distance between any two points, $\underset{\sim}{x}_i$ and $\underset{\sim}{x}_j$, in the random field and θ is the correlation length [11]. The same correlation length is used for all soil property fields. This is both for simplicity and because there is some rationale to the idea that if one soil property fluctuates due to changes in the soil makeup, it is likely that the other soil properties will fluctuate similarly. The use of isotropic random fields to represent the ground, rather than anisotropic fields, does not particularly affect the results of this research because resistance factors are primarily dependent on overall variability seen by the foundation. The horizontal versus vertical fluctuations and averaging details are not as important to the variability seen by the foundation, although they can have a significant influence on the mean foundation response and capacity. Because resistance factors are primarily affected by variability, not the mean, the assumption of isotropy is expected to make little difference.

Realizations of the random soil property fields are produced using one of the following methods for each problem considered in this research:

1. Local average subdivision (LAS): where the soil property field is used as input to a finite element model, the two-dimensional random field is simulated using the LAS technique [13]. The combined LAS and FE analysis is commonly referred to as the RFEM [9], [10]. LAS is used in the shallow foundation and retaining wall studies presented in this research.
2. Covariance matrix decomposition: when the random soil property field consists of a relatively small number of points in the field (e.g., less than 100), these points can be directly simulated using the covariance matrix decomposition method (see [11]). This method is used in the pile design studies presented in this research.

2.2 Random Load Models

The NBC [1] provides five ultimate limit state (ULS) load combinations regarding the relatively static dead load, F_D, lifetime maximum live load, F_L, snow load, F_S, seismic load, F_E, and wind load, F_W, as listed in Table 1.

This research is primarily concerned with load combinations 2 (without companion loads), 4 (for

Table 1: Load Combinations for Ultimate Limit States

Case	Principal load combinations	Companion load combinations
1	$1.4F_D$	—
2	$1.25F_D + 1.5F_L$	$1.0F_S$ or $0.4F_W$
3	$1.25F_D + 1.5F_S$	$1.0F_L$ or $0.4F_W$
4	$1.25F_D + 1.4F_W$	$0.5F_L$ or $0.5F_S$
5	$1.0F_D + 1.0F_E$	$0.5F_L + 0.25F_S$

wind loading), and 5 (for seismic loading). The loads are generally considered to be lognormally distributed single random variables that are independent of one another, with the exception of seismic design of piles, which uses covariance matrix decomposition to simulate correlated loads. The means of the load types considered in this research are taken as the characteristic design values times a bias factor. For example, the mean live load is taken as $\mu_L = k_L \widehat{F}_L$ and the mean dead load as $\mu_D = k_D \widehat{F}_D$, where $k_L = 0.95$ and $k_D = 1.05$ are the live and dead load bias factors, respectively [14]. For other load types, the means are taken to be equal to the characteristic design values. Reasonable estimates of the coefficients of variation of the various load types are taken from the literature and are discussed in Section 3. The individual loads are simulated by first simulating a standard normal random variable (using the radial transform method, see [11]) and then using Eq. (2) to transform to the appropriate lognormally distributed load (using the appropriate μ_{lnF} and σ_{lnF} parameters).

3 Target Maximum Acceptable Failure Probabilities

Before the resistance factors can be estimated, the target maximum acceptable failure probabilities (or, equivalently, the target reliabilities) for each limit state and geotechnical system need to be known, at least approximately. This is difficult because most structural designs are unique to their local site conditions, so assessing their actual reliability is virtually impossible. Because the estimation of a probability uses the frequency interpretation, where the probability of an event occurring is the number of times the event occurs divided by the number of trials, as the number of trials goes to infinity, this approach cannot be used as there is usually only one trial, the current design.

Instead, to estimate target maximum acceptable failure probabilities, p_m, this research uses estimates derived from the literature, which are typically based on the observed fraction of failures that current design approaches yield.

Esposito and Fenton [15] compared the reliability levels achieved by various geotechnical design standards. Their work was performed largely in terms of the so-called reliability index, β, which is related to the probability of failure, p_f, as

$$p_f = \Phi(-\beta), \tag{5}$$

where Φ is the standard normal cumulative distribution function. Distinction must also be made between the annual reliability index, β_1, and the *n*-year reliability index, β_n, because reliability typically decreases as the timespan increases. If years are considered to be independent trials, then $\Phi(\beta_n) = \Phi^n(\beta_1)$, so that

$$\beta_n = \Phi^{-1}[\Phi^n(\beta_1)] \quad \Leftrightarrow \quad \beta_1 = \Phi^{-1}\left[\Phi^{1/n}(\beta_n)\right] \tag{6}$$

For shallow foundations, Esposito and Fenton [15] derived the reliability results shown in Figure 1. The bias factor shown in these figures, $\lambda_R = \mu_R/\widehat{R}$, is the ratio of the mean resistance, μ_R, to the characteristic design resistance, $\widehat{R}$. In general, because characteristic soil properties tend to be conservatively selected, the predicted characteristic resistance tends to be less than the true mean resistance, $\widehat{R} < \mu_R$, so that λ_R would tend to be greater than 1.0. The results are also shown for various coefficients of variation of the ground resistance, COV_R.

Esposito and Fenton [15] estimated that the $n = 50$ year lifetime reliability index targets are around $\beta_n = 3.8$ in Europe and Australia, and around $\beta_n = 3.0$ in North America. For simplicity, β_n is referred to as β in the following.

For the same COV_R, Australian Standard (AS) 4678–2002, *Earth-retaining structures* [16], produces the most reliable (largest β) and most robust (able to meet the target with the largest COV_R) design, and the target reliability is met when $\lambda_R = 0.8$ and $COV_R = 0.3$. For the same COV_R, CSA S6:19, *Canadian highway bridge design code* (CHBDC) [17] and the *American Association of State Highway and Transportation Officials (AASHTO) LRFD bridge design specifications* [18] produce a robust design when $\lambda_R = 0.8$ and $COV_R = 0.25$, but the reliability levels of these two codes are the lowest. The European Standard (EN) 1997 Design Approach 1 (EN 1997 DA1) [3] produces the least robust design, only meeting the target reliability level when COV_R is less than about 0.2.

Figure 1: Lifetime reliability indices for shallow foundations achieved by the indicated codes versus the coefficient of variation of the resistance for a range of resistance bias factors. (a) CHBDC, (b) AASHTO, (c) EN 1997 DA1, (d) EN 1997 DA2, (e) AS 4678.

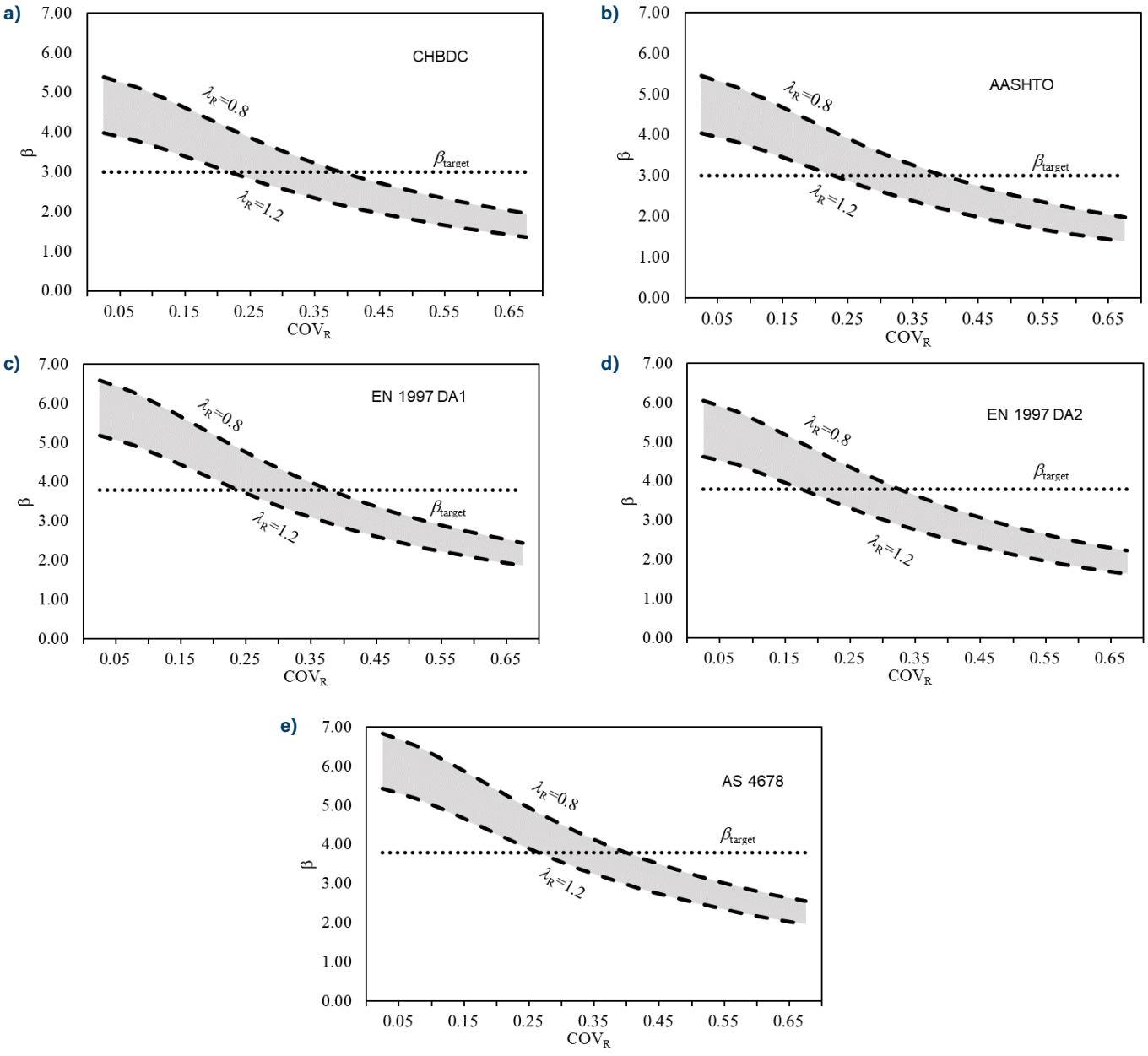

Esposito and Fenton [15] developed similar results for the target reliabilities of deep foundations, as shown in Figure 2. AASHTO (Figure 2b) and AS 2159–2009, *Piled footings design & installation* (Figure 2f), followed by CHBDC (Figure 2a) are the standards that produce the most robust designs. When considering their respective reliability targets, AASHTO and CHBDC have a higher chance of meeting the targets. With λ_R as high as 1.2, AASHTO meets the reliability target until COV_R exceeds 0.25, whereas CHBDC meets the reliability target until COV_R exceeds 0.20. With a λ_R of 0.8, CHBDC meets the reliability target until COV_R

Figure 2: Lifetime reliability indices for deep foundations achieved versus the coefficient of variation of the resistance for a range of resistance bias factors. (a) CHBDC, (b) AASHTO, (c) EN 1997 DA2, (d) EN 1997 DA1 UK-NA, (e) EN 1997 DA2 IR-NA, (f) AS 4678.

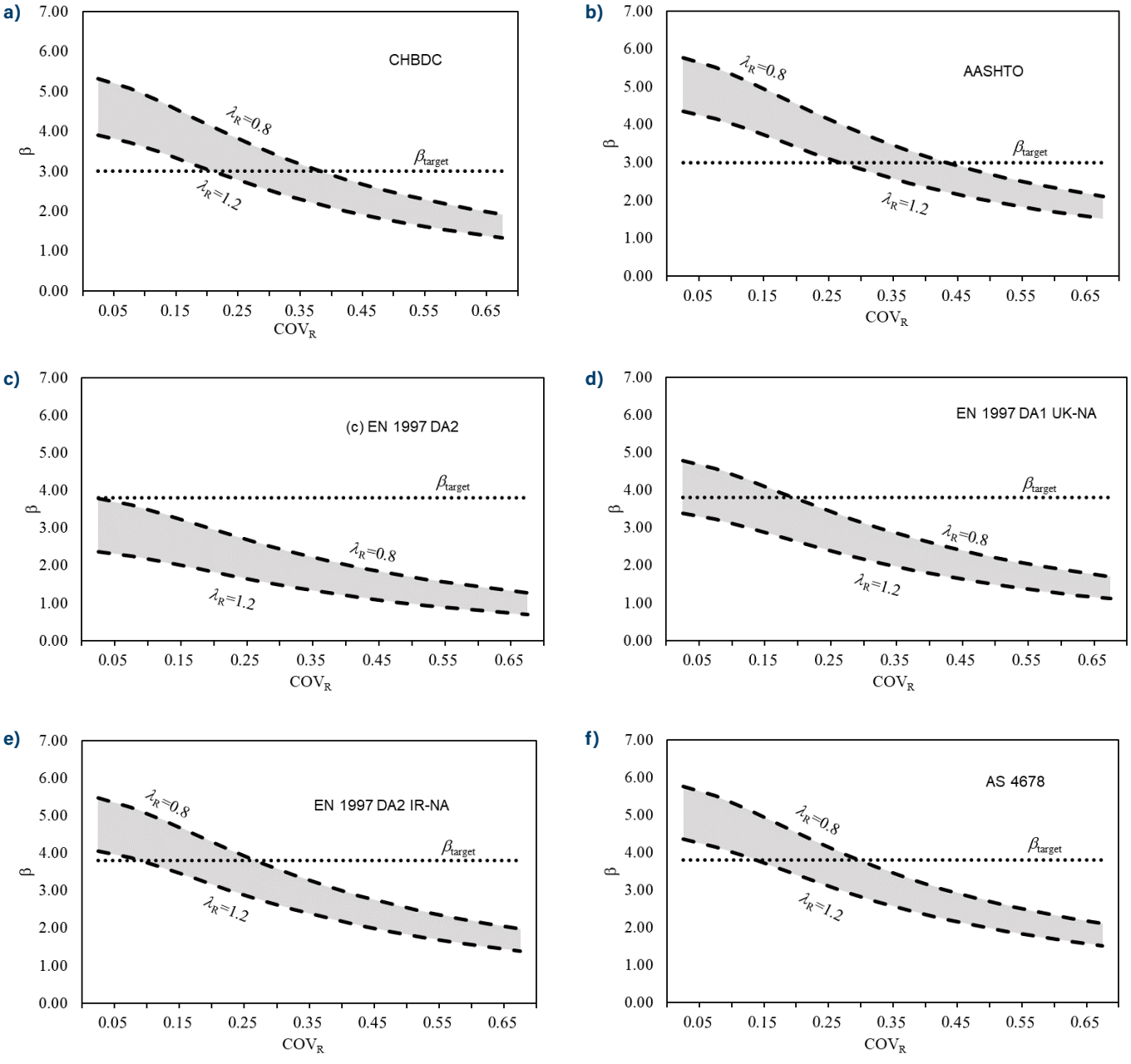

exceeds about 0.35, confirming its robustness, which was calibrated using a resistance variability of 0.15. Figure 2c shows that the EN 1997 Design Approach 2 (EN 1997 DA2) never achieves its target reliability level irrespective of the design approach λ_R. When using EN 1997 DA1 UK-NA (Figure 2d), if COV_R exceeds 0.2, the design cannot achieve its target reliability level, irrespective of λ_R.

If reasonable values of $COV_R = 0.3$ and $\lambda_R = 1.2$ are selected, the results in Figure 2 suggest a tendency to achieve actual lifetime reliability indices that are below — sometimes considerably below — their annual targets (which are about $\beta = 3.8$ in Europe and Australia and about $\beta = 3.0$ in North America). Nevertheless, it appears that in North America, a lifetime reliability index in the range of 2.5 to 3.0 is achieved.

Esposito and Fenton [15] did not consider the effects of geotechnical redundancy on overall system reliability. If a structure is founded on several deep foundations and the failure of a single foundation will not result in failure of the supported structure, then the geotechnical support system has redundancy and is safer than its individual components (piles). When a geotechnical support system has redundancy built into it, the target reliability index for the individual components can be lower. Previous calibration studies, such as Ref. [19], adopted a lifetime target reliability between 2.0 and 2.5 for redundant deep foundations. It is believed that similar targets can be adopted for redundant shallow foundations (although redundancy in shallow foundations is likely less common).

Because the effects of redundancy on overall system reliability can be large, there have been a number of studies to investigate these effects. One study by Naghibi and Fenton [20] suggested that for a lifetime system reliability index target of $\beta = 3.0$, the reliability index target for an individual pile (assuming that a "failed" pile can still support some load) will range from about $\beta = 2.3$ to $\beta = 2.5$.

In summary, for non-redundant geotechnical systems, a lifetime target reliability index of about $\beta = 3.0$ seems to be societally acceptable. For redundant geotechnical systems, the lifetime target reliability index for individual geotechnical components can be significantly reduced to the range of 2.0 to 2.5.

4 Random Finite Element Method Optimization

This section focuses on optimizing the computational cost of reliability-based analyses using parallel computing. This research uses the RFEM [11] to perform the reliability-based analysis. The bottleneck in RFEM analysis is the computational cost of the algorithm. In an RFEM algorithm, the finite element model is run thousands of times to help predict the distribution of the resistance. This can take months or even years on a personal computer, depending on the complexity of the problem. Because the finite element analyses in RFEM use separate input data for each model, while repeating the same analysis procedure, it is the perfect candidate for parallelizing using either central processing units (CPUs) or graphics processing units (GPUs).

Figure 3: 3-D finite element model of a soil mass.

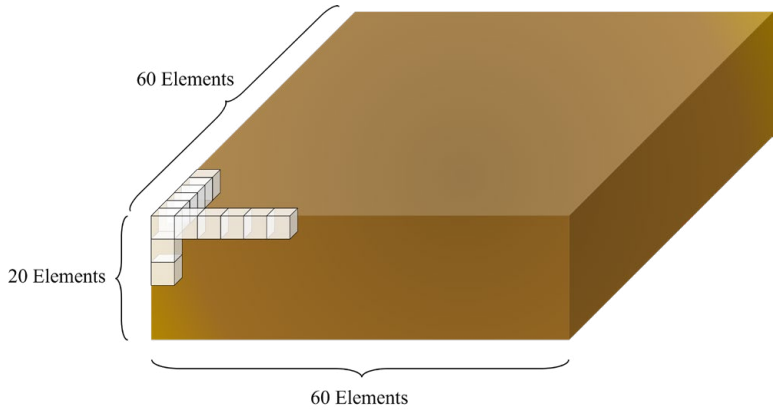

The amount of memory required to save the assembled stiffn ss matrix can slow down the finite element process considerably. In modern computers, there are three common types of memory devices: the CPU cache (very fast), random access memory (RAM, reasonably fast), and solid state drives (SSD, relatively slow). The size of the memory modules for these devices is in the order of megabytes (MB), gigabytes (GB), and terabytes (TB), respectively. As the size increases, the read and write speed of the memory decreases substantially. In a complex finite element analysis, the assembled stiffn ss matrix will not usually fit in the fastest memory modules, which results in a performance penalty. Assembling the stiffn ss matrix can also prevent running multiple finite element realizations at the same time as there might not be enough available memory. For example, Figure 3 shows a soil mass that might underly a shallow foundation, modelled using three-dimensional elements. In this finite element model, the soil mass has been discretized into 60 by 60 by 20 elements in the *x, y* (horizontal), and *z* (vertical) directions, respectively. The total number of elements used in this model is thus 72 000 and the assembled stiffn ss matrix requires 409 GB of memory, which cannot fit on the CPU cache, probably will not fit on RAM, and may not fit on an SSD. The larger memory modules required to store this matrix will impose a severe runtime penalty.

For this research, a matrix-free (assembly-free) approach was developed to avoid assembling and storing the global stiffn ss matrix. This method substantially reduces the amount of memory required but it also increases the processing load. However, the extra processing load is less expensive than the memory speed bottleneck. In the matrix-free approach, the conjugate gradient method is used to solve the system of equations element by element [21]. Consequently, only a vector the size of the free degrees of freedom needs to be saved in memory. The memory required for the example shown in Figure 3 is 10 MB, which will easily fit in RAM and may fit in the CPU cache. At the time of writing, the average size of RAM space in a personal computer ranges between 8 to 24 GB.

Next, the steps taken in the finite element method are parallelized to form and assemble the stiffn ss matrix, and then to solve the resulting system of equations. The details of this research are presented in Rahimi et al. [22]. Only the results are discussed in this research. Figure 4 compares the total runtime of the finite element model in the serialized and the proposed parallel algorithms. In a workstation equipped with 128 CPU threads, 128 GB of RAM, and an Nvidia Titan Xp GPU, the proposed parallel algorithm completed the running of 1000 finite element realizations in 17.4 ms. The same set of realizations took 1000.45 ms using the traditional serial algorithm. These results show that the proposed parallel algorithm completed 1000 finite element realizations 57 times faster than the traditional serial algorithm.

Figure 4: Performance comparison of the serial and parallel algorithms.

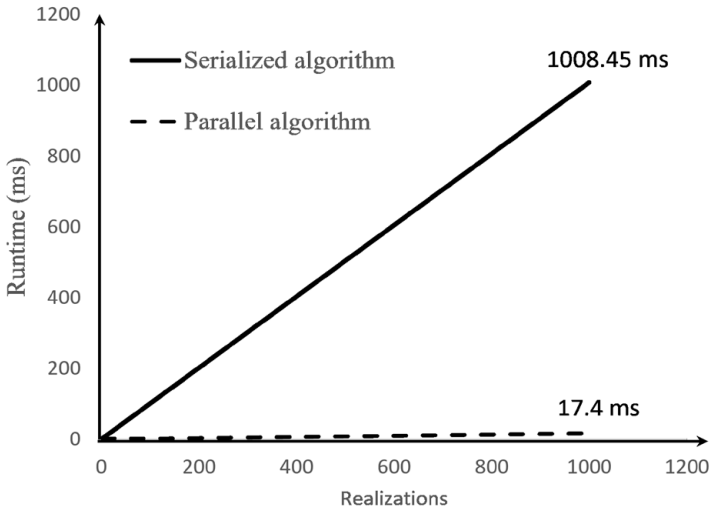

5 Seismic Loading Design of Deep Foundations

Esposito et al. [23] studied the seismic performance of piles with respect to settlement. Their investigation into current provisions for the seismic loading design of deep foundations suggested that the recommended resistance factors in current Canadian design codes are too high, resulting in failure probabilities that exceed target maximum acceptable failure probabilities, p_m, or, equivalently, reliability indices that are too low. Because few geotechnical failures due to seismic loading have been observed in Canada in the last several decades, Esposito et al. [23] may have been overly conservative in not considering the additional safety provided by redundant geotechnical systems (i.e., multiple piles) or it may simply be that Canada has not experienced any large earthquakes recently. It could also be that this study ignores structural seismic detailing of fuses and ductile elements, in certain circumstances, which may provide additional safety.

As part of this research, Esposito and Fenton [24] investigated the effects of redundancy and soil–structure interaction. The results are summarized here.

Determining the reliability levels achieved by foundation systems subjected to seismic loads is a complicated task due to the highly non-linear soil response, the soil variability, and the uncertainty of the seismic hazard. The beneficial effects of structural rigidity on foundation performance are often ignored in an attempt to keep the problem simple, based on the perception that this will produce "conservative" results. While this approach may be justified from a safety perspective, it creates challenges when attempting to quantify performance levels achieved by the foundation system under seismic loads. In addition to the effects of structural rigidity and capacity protected design, other sources of uncertainty, such as the uncertainty of the seismic hazard and of the geotechnical model, make it difficult to quantify seismic foundation performance. The degradation of soil properties during seismic events adds an additional degree of complication to the rigorous analysis of the problem. Due to these challenges, with LRFD design the geotechnical resistance factor for the seismic case is usually assigned a value based on "common sense" rather than on a rigorous probabilistic calibration.

With the ultimate goal of estimating fully calibrated geotechnical resistance factors for the seismic case, the reliability level achieved by non-redundant vertical piles subject to seismic load is investigated here through a simplified approach that includes:

1. the effect of the foundation-structure interaction;
2. the modeling of the non-linear soil properties and of the structural loads as random fields;
3. the Canadian seismic hazard levels [25] and their variability for the cities of Vancouver and Montreal; and
4. the NBC provisions [1] for the calculation of the seismic forces transmitted from the structure to the pile foundation.

Considering the reliability targets adopted for the design of geotechnical systems under static dead and live loads, this research investigates whether seismic geotechnical design according to the NBC provisions [1] achieves reliability levels similar to those targeted for static design over the design life.

5.1 Site Characteristics

A model of the site conditions considered in this research, shown in Figure 5, includes a saturated 30 m thick layer of silty sand (site class D) with an average shear wave velocity of 250 m/s overlying the half space corresponding to site class B with an average shear wave velocity of 1100 m/s. The average shear wave velocities correspond to those used for the site effect factors [26] in the NBC [1]. Note that the site classification depends on its liquefaction susceptibility. For example, the same site could be classified as F in parts of Canada where the ground motion hazard is able to cause liquefaction, in which case the simplified equivalent static force procedure (ESFP) approach could not be used. This research simplifies the problem and applies the ESFP approach where liquefaction may occur because it is nevertheless a reasonable approximation. Under seismic conditions, the degraded soil pile design parameters are derived from the excess pore pressure following the procedure used in Esposito et al [23].

Figure 5: Reinforced concrete frame, pile foundation, and site considered in this research.

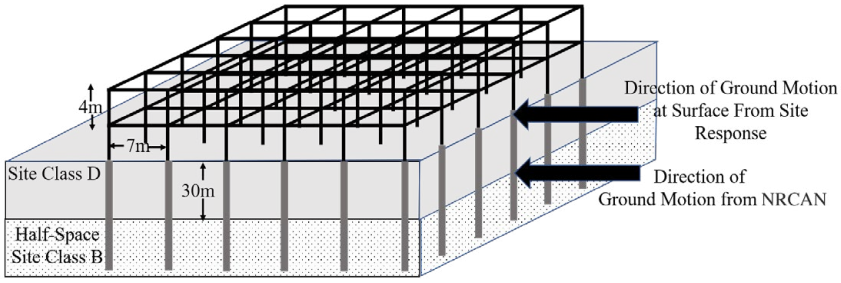

5.2 Structural Model

The structural response is calculated using conventional matrix analysis techniques through the stiffn ss method. The structural geometry selected for this research is a reinforced concrete bare frame of moderate ductility (see Figure 5). The structure, a five-bay, two-story frame, was used by Al Mamun and Saatcioglu [27] to generate fragility curves for moderately ductile buildings in Eastern Canada using hysteretic models with different features reflecting the recommendations of different North American standards. It is important to highlight that reinforced concrete structures on the West Coast of Canada use other mechanisms to increase their seismic resiliency. Other details on the structural characteristics of the selected frame are available in Ref. [27] and will not be repeated here.

For ULS static load conditions, the NBC [1] is based on $\beta_{50} = 3.0$, which approximately corresponds to $\beta_1 = 4.0$. While this research focuses on ULS performance, it is useful to understand how codes provide for serviceability limit state (SLS) conditions. The NBC [1] is not calibrated for SLS conditions, aside from assuming that all load and resistance factors are equal to 1.0, therefore, this research uses $\beta_{50} = 1.8$, which is specified in the EN 1997 [3] for SLS. In terms of target deformations, using a bay length of 7 m and considering that the building is of normal (typical) importance, the ULS settlement limit is 140 mm. For SLS, the settlement limit is assumed to be 25 mm. The results for the different design cases are shown below. For each realization of the hazard, two examples of the regression of the settlement versus the spectral acceleration and of the fragility curves considering 50 mm and 200 mm as limit settlements and the annual reliability index, are presented.

Figure 6 and Figure 7 show the results for Montreal and Vancouver, respectively, where the seismic loads govern, the geotechnical resistance factor, ϕ, is 1.0, and the piles are designed using load combination 5.

Figure 6: Montreal — Piles designed with static load combination 5 and ϕ = 1.0; (a) ground motion hazard; (b) Limit state function; (c) pile conditional probability of failure; (d) calculated reliability index.

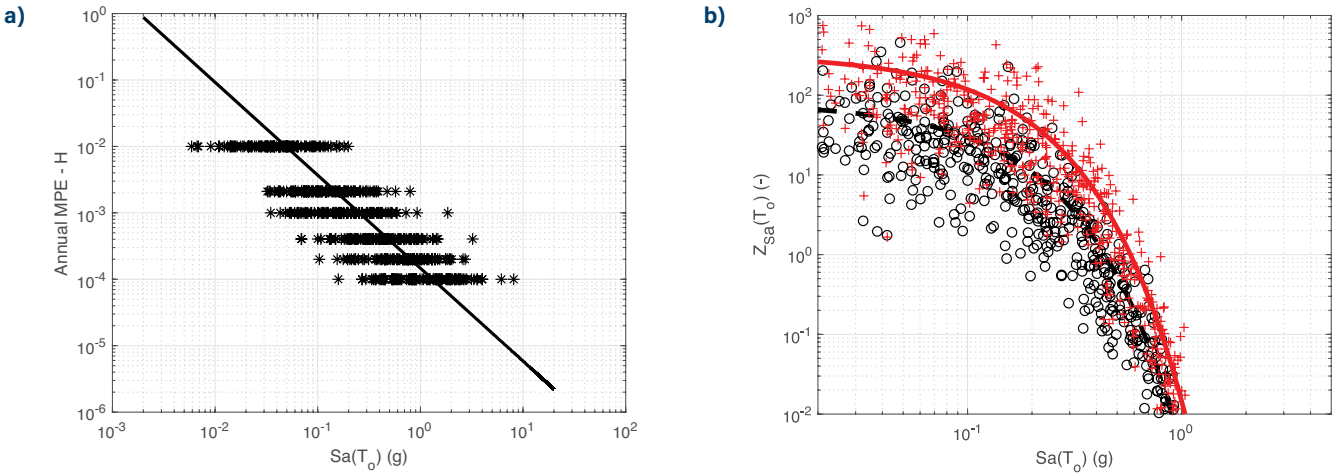

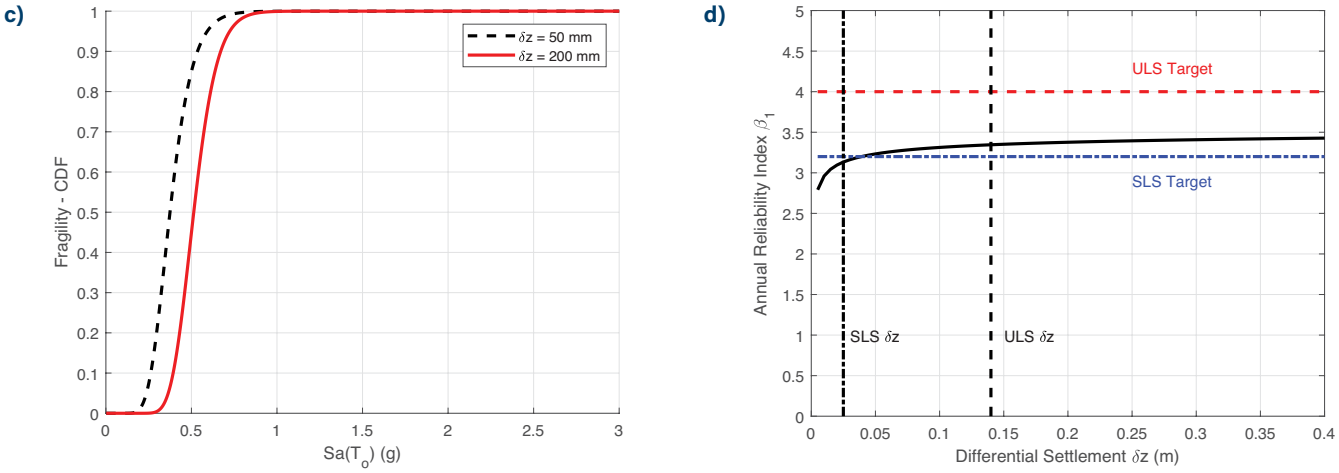

Figure 7: Vancouver — Piles designed with static load combination 5 and $\phi = 1.0$; (a) ground motion hazard; (b) Limit state function; (c) pile conditional probability of failure; (d) calculated reliability index.

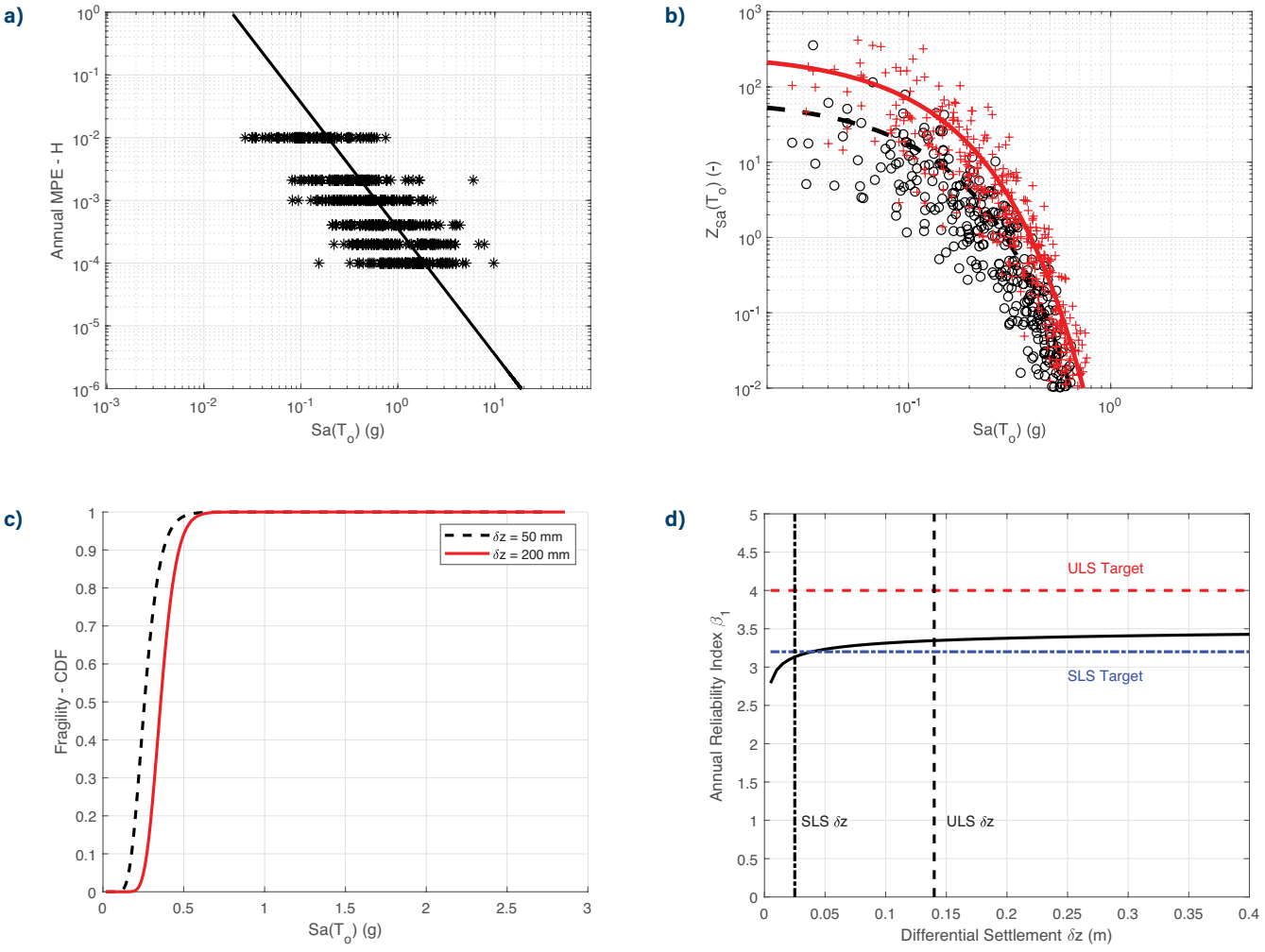

The different slope of the hazard (Figures 6a and 7a) between Vancouver and Montreal has a limited impact on the regression of the limit state function Z (Figures 6b and 7b) and on the fragility of the foundation $F_Z(a)$ (Figures 6c and 7c). In Vancouver, a few more Z values fall below the failure line, $Z = 1$, than in Montreal. As a consequence, the Vancouver fragility curves $F_Z(a)$ (Figure 7c) are slightly steeper than those in Montreal, indicating a higher conditional probability of failure. The calculated ULS reliability indexes in both Montreal $(\beta_{ULS,1} = 3.3)$ and Vancouver $(\beta_{ULS,1} = 2.7)$ are below the target $(\beta_{ULS,1} = 4)$. The estimated SLS reliability indexes are also below the targets for both cities.

Figure 8 and Figure 9 show the results for Montreal and Vancouver, respectively, for cases where the static loads govern and the piles are designed using load combination 2 with a geotechnical resistance factor, ϕ, of 0.4. In these cases, the different slopes of the hazard (Figures 8a and 9a) between Vancouver and Montreal have a limited impact on both the regression of the settlement limit state function Z (Figures 8b and 9b) and the fragility of the foundation $F_Z(a)$ (Figures 8c and 9c). The fragilities $F_Z(a)$ are now gentler and the resulting pile reliability is higher. The estimated reliability index $(\beta_{ULS,1} = 3.9)$ at the ULS conditions is now very close to the target $(\beta_{ULS,1} = 4)$ in Montreal, whereas it is still slightly less than the target in Vancouver $(\beta_{ULS,1} = 3.75)$ due to the probability of liquefaction at shorter return periods. The SLS target reliability is met in both Montreal and Vancouver.

Figure 8: Montreal — Piles designed with static load combination 2 and $\phi = 0.4$; (a) ground motion hazard; (b) Limit state function; (c) pile conditional probability of failure; (d) calculated reliability index.

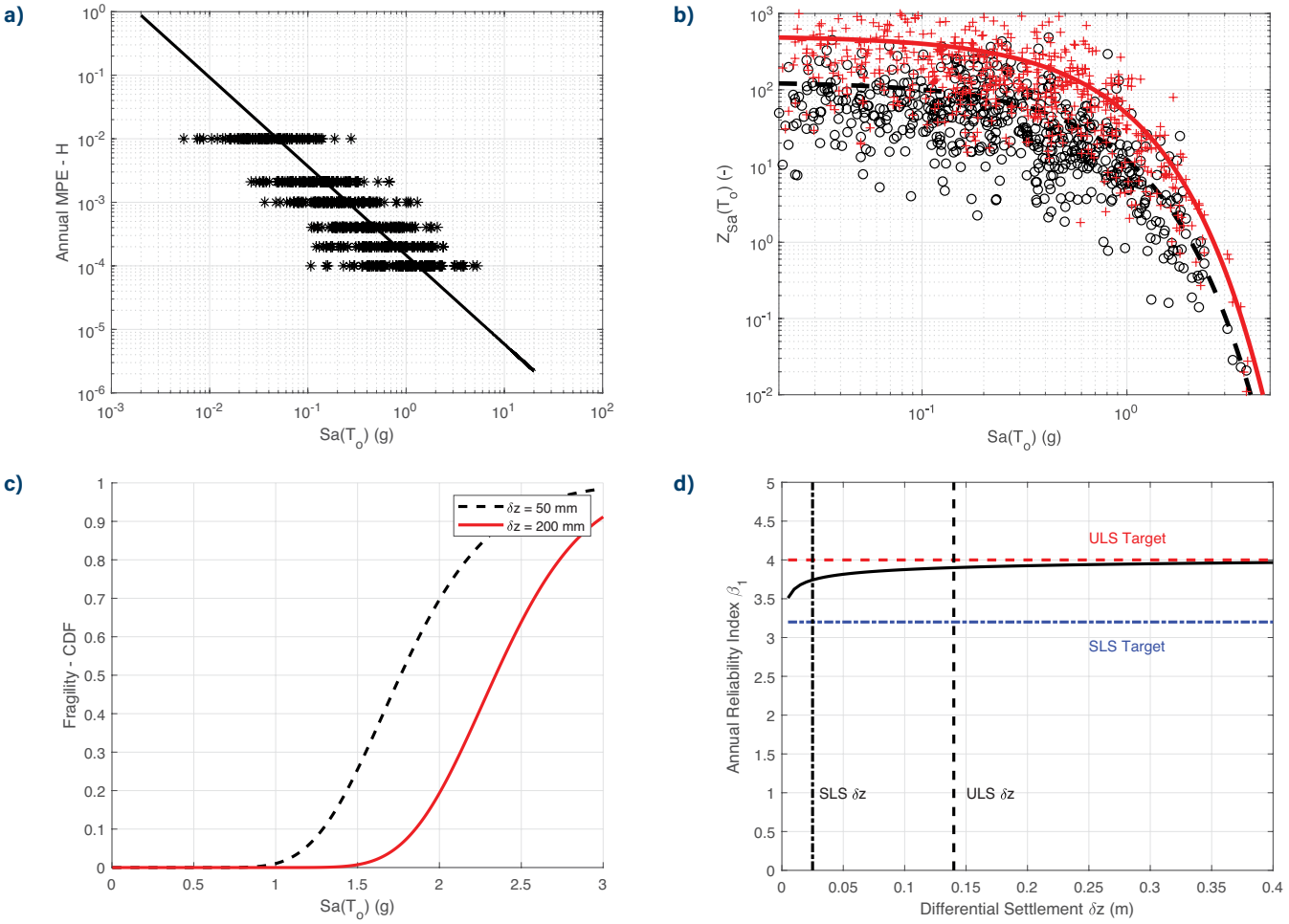

Figure 9: Vancouver — Piles designed with static load combination 2 and ϕ = 0.4; (a) ground motion hazard; (b) Limit state function; (c) pile conditional probability of failure; (d) calculated reliability index.

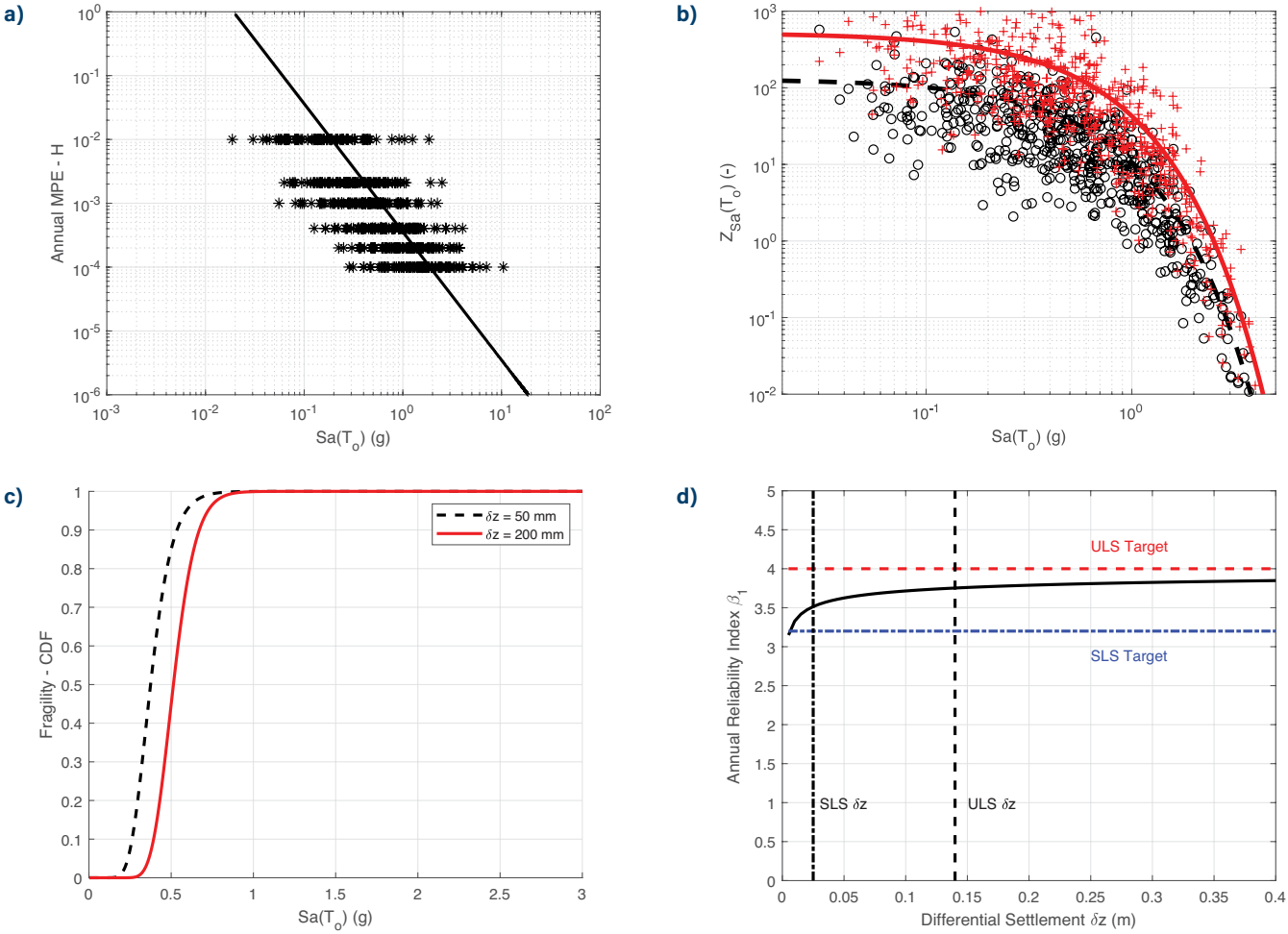

In both Montreal and Vancouver, piles designed using a geotechnical resistance factor of $\phi = 1.0$ do not achieve either the ULS or the SLS target reliability levels. When using a geotechnical resistance factor of $\phi = 0.4$ (static geotechnical resistance factor), the calculated ULS reliability index in Montreal is 3.9 and in Vancouver is 3.4, which are both closer to the reliability target $(\beta_{ULS,1} = 4)$, especially in Montreal. With the geotechnical resistance factor of $\phi = 0.4$, the SLS reliability target $(\beta_{ULS,1} = 3.2)$ is largely exceeded. Interestingly, the British Columbia Building Code 2018 (BCBC) [28] requires a geotechnical resistance factor of $\phi = 0.7$ for elements that are not capacity protected, but that still seems insufficient to achieve the reliability target.

6 Seismic and Wind Loading Design of Shallow Foundations

In this section, the resistance factors required for the bearing capacity design of shallow foundations under seismic and wind loading are estimated. The details of this research can be found in He et al. [29]. For simplicity, and to convert the soil model used into a two-dimensional random field, a strip foundation is considered under the NBC's load combination 4 for wind loading and 5 for seismic loading. The design phase uses the general bearing capacity equation for shallow foundation design, as specified in the CHBDC [17],

$$q_u = s_u N_c s_c d_c i_c + q N_q s_q d_q i_q + 0.5\gamma' B N_\gamma s_\gamma d_\gamma i_\gamma, \quad (7)$$

where s_u is the soil undrained shear strength; q is the surcharge pressure; γ' is the unit weight of soil; B is the foundation width; s_c, s_q, and s_γ are the foundation shape factors; d_c, d_q, and d_γ are the foundation depth factors; i_c, i_q, and i_γ are the load inclination factors; and N_c, N_q, and N_γ are the bearing capacity factors, depending only on the soil effective internal friction angle, ϕ'. For strip foundations (i.e., $s_c = s_q = s_\gamma = 1$) with zero embedment depth (i.e., $d_c = d_q = d_\gamma = 1$) and zero surcharge (i.e., $q = 0$), Eq. (7) reduces to the following, with the hat parameters used for foundation design,

$$\hat{q}_u = \hat{s}_u \hat{N}_c i_c, \quad (8a)$$

for undrained (purely cohesive) soil conditions,

$$\hat{q}_u = 0.5\gamma' \hat{B} \hat{N}_\gamma i_\gamma, \quad (8b)$$

for drained (purely frictional) soil conditions,

where $\hat{q}_u$ is the characteristic ultimate bearing resistance (in units of pressure), and the bearing capacity factors and load inclination factors recommended by the CHBDC [17] are used.

For a given resistance factor, ϕ_{gu}, the total bearing capacity failure probability of the strip foundation can be approximated using the sum of a finite number of terms in the total probability theorem,

$$p_f \approx \sum_{i=1}^{n} \boldsymbol{P}[F_T > \bar{R}_u | E = e_i] \cdot \boldsymbol{P}[E = e_i], \quad (9)$$

where F_T is the actual vertical load experienced during an earthquake or wind event; $\bar{R}_u$ is the actual ultimate vertical resistance of the designed foundation; and e_i is a seismic or wind event.

A seismic event is characterized by the earthquake return period, *r,* and a wind event is described by the annual maximum hourly average wind speed, *v,* also associated with a return period, *r.* Eq. (9) can thus be written specifically for seismic and wind loading conditions as

$$p_f \approx \sum_{i=1}^{n} \boldsymbol{P}[F_T > \bar{R}_u | R = r_i] \cdot \boldsymbol{P}[R = r_i], \quad (10a)$$

for seismic loading conditions,

$$p_f \approx \sum_{i=1}^{n} \boldsymbol{P}[F_T > \bar{R}_u | V = v_i] \cdot \boldsymbol{P}[V = v_i], \quad (10b)$$

for wind loading conditions.

The details of the estimation of the conditional failure probability and the unconditional probability shown in Eq. (10) are provided in He et al. [29].

For the Monte Carlo simulation, the RFEM [9], [10] is used to estimate the conditional bearing capacity failure probability of the strip foundation for each return period wind or seismic event. Specifically, the "rbear2d" program developed by the authors was modified for this research to include horizontal loading and to estimate the bearing capacity failure probability of the designed shallow foundation under combined vertical and horizontal loading. The program employs a two-dimensional plane strain finite element model of the ground [21] to predict the actual bearing resistance of each of a series of realizations of the ground property random fields, each generated using LAS [13]. The finite element model uses an elastic-perfectly plastic soil constitutive model with a Mohr-Coulomb failure criterion. The foundation is assumed to be rigid and rough. The finite element mesh consists of 7680 eight-node quadrilateral elements (120 elements wide by 64 elements deep) and each element is a 0.1 × 0.1 m square.

Figure 10 illustrates a typical deformed mesh of the finite element model at foundation bearing failure for a soil with spatially varying properties. Lighter regions in the figure indicate soils with lower strength properties (s_u or ϕ'). It should be noted that, due to spatial variability, the failure mechanism is no longer symmetric [12], as traditionally predicted by the bearing capacity theory developed for homogeneous soils [30].

In this research, a simple five-storey office building (6 m wide and 5 × 3 m in height) supported by two strip foundations is taken as an example, as shown in Figure 11. For seismic loading conditions, each foundation is assumed to resist half of the total load (i.e., the sum of dead, live, seismic, and snow loads) acting on the structure. For wind loading conditions, the foundation reactions (i.e., vertical and horizontal loads) are evaluated using the software SAP2000 [31], assuming a concrete structural frame. Preliminary analyses showed that the leeward foundation of the structure is the worse case, having the highest probability of bearing capacity failure, and thus only the leeward foundation is considered for wind analysis (see Figure 11).

Figure 10: Typical deformed mesh of the finite element model at bearing failure for a soil with spatially varying properties.

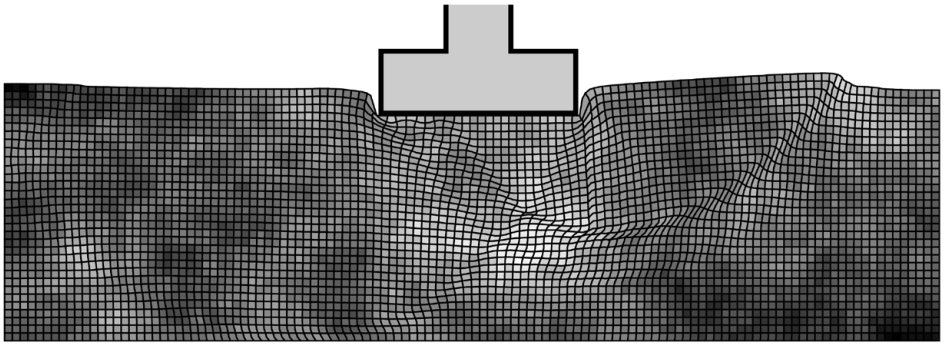

Figure 11: Schematic example building and load distributions for wind loading conditions.

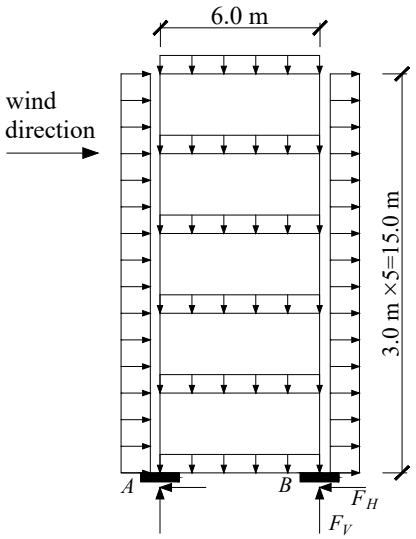

The building is assumed to be located in two Canadian cities, for each loading condition, to investigate the effects of load statistics on the resistance factors: Toronto and Halifax for wind loading, and Toronto and Vancouver for seismic loading.

The live load acting on each floor in the example can be obtained from the NBC [1], and the dead load is taken as three times the live load [32]. The dead load is assumed to have a coefficient of variation, $\nu_D = 0.15$ [5], and the live load is expected to be more variable with $\nu_L = 0.3$ [6], [7]. As the intensity of seismic loads also depends on the total mass of the structure, a larger coefficient of variation of $\nu_E = 0.85$ is assumed for the seismic load [33]. The coefficient of variation of the snow load is taken as $\nu_S = 0.5$ [34], while the coefficient of variation of the wind load acting on the structure is taken as $\nu_W = 0.3$ [35]. As mentioned above, the dead, live, seismic, and snow load factors are taken as $\alpha_D = 1.0$, $\alpha_L = 0.5$, $\alpha_E = 1.0$, and $\alpha_S = 0.25$ for the seismic load combination (ULS case 5 in the NBC, see Table 1); the dead, live, and wind load factors are taken as $\alpha_D = 1.25$, $\alpha_L = 0.5$, and $\alpha_W = 1.4$ for the wind load combination (ULS case 4 in the NBC, see Table 1).

The parameters considered for the Monte Carlo simulations performed for this research are shown in Table 2. The ϕ' random field for drained soil conditions is assumed to have a mean of 35° and a standard deviation of 3.4°. The mean and standard deviation of the s_u field are assumed to be 100 and 50 kPa. That is, the coefficient of variation of s_u is assumed to be $\nu_{s_u} = 0.5$, which is conservatively at the upper end of the range of $\nu_{s_u} = 0.2$ to 0.5 reported by Lee et al. [36]. The correlation lengths of s_u and ϕ' are assumed to be the same as the distance of the soil sample location from the foundation centerline, $s = \theta$, because this is also conservative, giving the highest failure probability [37].

In the parametric study carried out for seismic loading conditions, the design earthquake return period is assumed to be r_d = 0, 475, 975, and 2475 years. The value r_d = 0 indicates that seismic loads are not considered in the foundation design. The design wind speeds specified by the NBC [1] can be found from Table 2. All the other parameters are held constant, as tabulated in Table 2. Monte Carlo simulations are performed for each case. The simulation involves 1000 realizations of the soil property random fields and

Table 2: Input Parameters for Monte Carlo Simulations

Parameters	Values
Soil undrained shear strength: μ_{s_u}, σ_{s_u} (kPa)	100, 50 (ν_{s_u} = 0.5)
Soil effective internal friction angle: $\mu_{\phi'}, \sigma_{\phi'}(^\circ)$	35, ≈3.4 ($\nu_{\phi'} \approx 0.1$)
Factors associated with seismic loads: $M_v, I_E, R_d R_o$	1.0, 1.0, 1.5
Design earthquake return period: r_d (years)	0; 475; 975; 2475
1-in-50-year snow and associated rain loads: S_s, S_r (kPa)	0.9, 0.4 for Toronto
	1.8, 0.2 for Vancouver
Factors associated with snow loads: I_s, C_b, C_w, C_s, C_a	1.0, 0.8, 1.0, 1.0, 1.0
Factors associated with wind loads: I_w, C_e, C_t, C_g, C_p	Windward: 1.0, 1.08, 1.0, 2.0, 0.8
	Leeward: 1.0, 1.08, 1.0, 2.0, –0.5
	Roof: 1.0, 1.08, 1.0, 2.0, –1.0
Load factors (seismic conditions): $\alpha_D, \alpha_L, \alpha_E, \alpha_S$	1.0, 0.5, 1.0, 0.25
Load factors (wind conditions): $\alpha_D, \alpha_L, \alpha_W$	1.25, 0.5, 1.4
Live load: μ_L, σ_L (kN/m)	43.9, 13.2 (ν_L = 0.3)
Dead load: μ_D, σ_D (kN/m)	131.7, 19.8 (ν_D = 0.15)
Soil sample distance and correlation length: $s = \theta$ (m)	3.0
Soil sample depth: L (m)	3.0
Soil unit weight: γ'(kN/m³)	20.0
Element size: $\Delta x = \Delta y$ (m)	0.1
Number of elements in horizontal and vertical directions: n_x, n_y	120, 64
Number of realizations: n_{sim}	1000

foundation loads and the subsequent finite element analyses. The conditional failure probabilities are approximated by $\frac{n_{fail}}{n_{sim}}$, where n_{fail} is the number of times the foundation fails and $n_{sim} = 1000$ is the total number of simulations.

Figure 12 shows the relationships between the total seismic failure probability and resistance factor for Toronto and Vancouver under both drained and undrained soil conditions. A target lifetime failure probability of $p_m = 1 \times 10^{-2}$, recommended by ASCE/SEI 7-16, *Minimum design loads* and associated criteria for buildings and other structures [38], is also superimposed to determine the required resistance factors. It should be noted that $p_m = 1 \times 10^{-2}$ is much greater than the target failure probability range for static foundation design recommended by Becker [6], [7] for the NBC [1]. This is deemed to be reasonable because a greater target failure probability is expected for seismic loading versus static loading due to the rarer nature of extreme loads. For example, CHBDC [17] specifies different target safety levels for static and seismic geotechnical design: a seismic geotechnical resistance factor of 1.0 can be used for capacity-protected elements using the performance-based design, and the static resistance factor plus 0.2 is applied for force-based design elements. In addition, CHBDC [17] explicitly allows for increased damage as the design earthquake return period increases, implying lower reliability targets for higher earthquake intensities. CFEM [2] also suggests a smaller factor of safety be adopted for the seismic design of foundations, which again suggests that lower reliability targets could be used.

As evident in Figure 12(a), the total failure probabilities for Toronto have a very small dependence on the design earthquake return period, r_d. The primary reason is that the seismic horizontal load evaluated

Figure 12: Total seismic bearing capacity failure probability for (a) Toronto and (b) Vancouver.

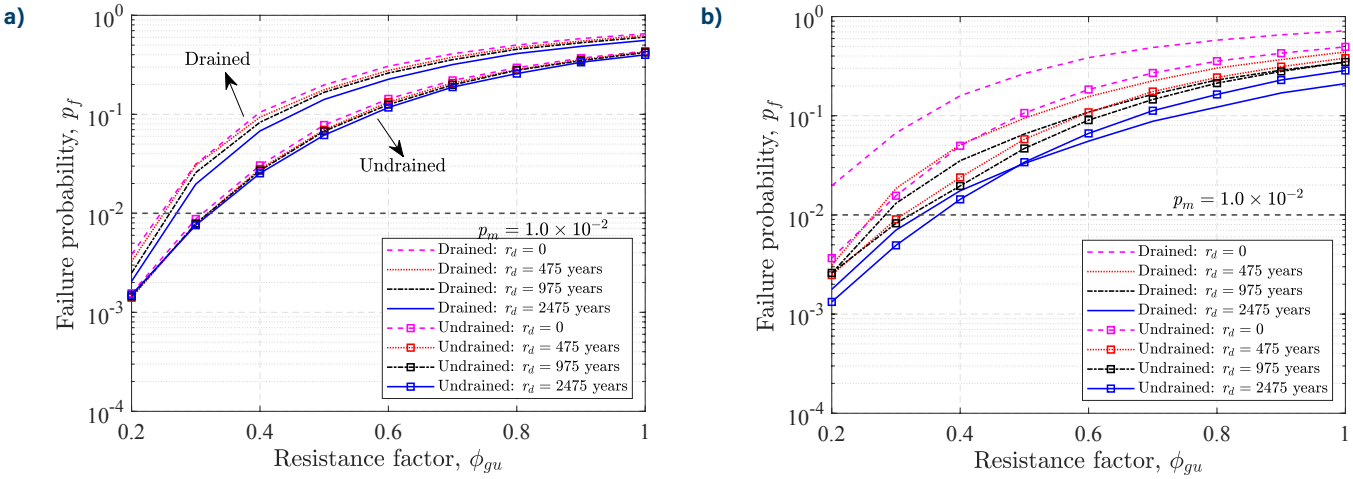

using r_d is much smaller than the total vertical load for Toronto. In comparison, the total failure probabilities for Vancouver appear to be relatively more dependent on r_d, as shown in Figure 12(b). This is because Vancouver is one of the most earthquake-prone cities in Canada, so the seismic horizontal load for Vancouver is expected to be greater than that for Toronto.

Figure 12(a) suggests that the failure probabilities under drained soil conditions are greater than those under undrained soil conditions, particularly for Toronto. This could be due to the fact that the bearing capacity factor, N_γ, used for foundation design under drained soil conditions involves more uncertainties, because N_γ is very sensitive to ϕ'. Alternatively, for undrained soil conditions, the bearing capacity factor, N_c, is basically deterministic (i.e., $N_c = \pi + 2$). For Toronto, using the curves for $r_d = 2475$ years, the resistance factors required to achieve this target failure probability are around 0.27 for drained soil conditions and 0.32 for undrained soil conditions. The required resistance factor for Vancouver is about 0.35 for both drained and undrained soil conditions.

The results indicate that the seismic resistance factors required for the target failure probability are lower than the value of $\phi_{gu} = 0.5$ recommended by the NBC User's Guide [8] for static foundation design. In other words, according to this reliability analysis, the current practice of foundation capacity design under seismic loading appears to be unconservative. However, it should be noted that the resistance factor prescribed by the NBC [1] was originally determined for static loads. Under seismic loading conditions, in many cases the foundation is allowed to be loaded closer to its ultimate resistance [23]. In addition, the target failure probability, $p_m = 1{\times}10^{-2}$, suggested by ASCE/SEI 7-16 [38] is targeted for system design rather than for a single foundation. Practical structures are usually supported by foundation systems, consisting of multiple individual foundations and possessing additional strength reserves. Therefore, a higher target failure probability is expected for a single foundation, and the resistance factor of $\phi_{gu} = 0.5$ recommended by the NBC User's Guide [8] for static foundation design is still likely to be achieved.

Figure 13 shows the relationships between the total wind bearing capacity failure probability and resistance factor for Toronto and Halifax under both drained and undrained soil conditions. Ellingwood and Tekie [39] considered a target annual failure probability of $7.0{\times}10^{-4}$. If it is assumed that annual extremes in loads and resistances from year to year are independent, then a 50-year target lifetime failure probability is given by $p_m = 1 - (1 - 7.0{\times}10^{-4})^{50} = 3.4{\times}10^{-2}$, which is of the same order of magnitude as that used for seismic loading. Therefore, the same target lifetime failure probability of $p_m = 1.0{\times}10^{-2}$ is also employed for wind loading conditions, as shown in Figure 13.

Figure 13: Total wind failure probability for Toronto and Halifax.

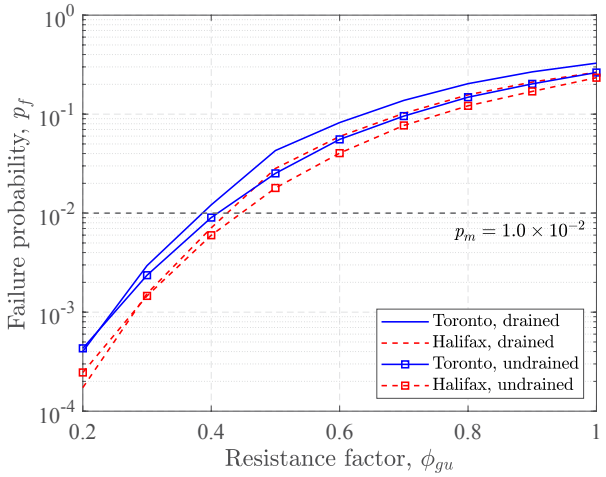

The resistance factors required to achieve the target failure probability range from 0.39 to 0.45, which is greater than the resistance factors required for seismic loading conditions. If the target failure probability of $p_m = 3.4{\times}10^{-2}$ [39] is used, the resistance factor required for wind loading seems to be better aligned with the static resistance factor of $\phi_{gu} = 0.5$ specified in the NBC User's Guide [8]. Considering redundant foundation systems used in practice, a resistance factor of $\phi_{gu} = 0.5$ could still be reasonable for wind loading conditions.

7 Sliding Resistance Design of Shallow Foundations

Limit states are classified into two primary categories: ULS and SLS. Based on CHBDC [17] and the CFEM [2], the key geotechnical ULS of shallow foundation design consists of bearing capacity failure and sliding failure. Compared to bearing capacity failure, studies on sliding failure of shallow foundations within the limit state framework are sparse. The aim of this section is to calibrate the geotechnical resistance factor for shallow foundations against ultimate sliding failure. This research only considers strip foundations, but the resistance factor is expected to be similar for other foundation shapes. The horizontal load on the foundation is assumed to be due to wind loads acting on the superstructure. Only the main findings are discussed here, but further details are available in He and Fenton [40].

For shallow foundation sliding, cohesive and frictional soils are separately considered because the physics affecting foundation sliding resistance for the two cases are different. The sliding resistance of shallow foundations on cohesive soils is determined only by the foundation dimension and the adhesion at the soil–foundation interface, but is unaffected by the vertical load on the foundation. In contrast, the sliding resistance of shallow foundations on frictional soils is associated only with the vertical load on the foundation and the effective internal friction angle at the interface, but is not influenced by the foundation dimension. Monte Carlo simulations are used to evaluate the sliding failure probability for cohesive soils, while an analytical method is developed for frictional soils.

The horizontal load for foundation sliding is considered to be wind loading. Assuming that the building is not dynamically sensitive, the wind loads can be evaluated using the Static Procedure provided by the NBC [1]. The external wind pressure or suction acting on a surface of the building is calculated using

$$p_W = I_w(0.5\rho v^2)C_e C_t C_g C_p, \tag{11}$$

where I_w, C_e, C_t, C_g, and C_p are the importance factor, exposure factor, topographic factor, gust effect factor, and external pressure coefficient, respectively; ρ is the density of dry air ($\rho = 1.2929$ kg/m^3 is normally used as an average value for wind pressure calculations); and v is the annual maximum hourly average wind speed.

Assuming that the building has uniformly distributed small openings amounting to less than 0.1% of the total surface area of the building, according to the NBC [1], the internal wind pressure or suction can be taken to be zero. Because the roof wind load (in the vertical direction) is much smaller than the dead and live loads, only external windward and leeward wind pressures (in the horizontal direction) are considered hereafter. Different values of the factors used in Eq. (11) are employed for external windward (p_{ww}) and leeward (p_{wl}) wind pressures. It should be noted that the total wind load, per unit length, acting on the strip foundations of the building is computed as

$$F_W = (p_{ww} - p_{wl})H, \tag{12}$$

where p_{ww} and p_{wl} are the external windward and leeward wind pressures on the structure computed using Eq. (11), respectively, and H is the building height.

The NBC [1] provides five ULS load combinations involving the relatively static dead load, lifetime maximum live load, snow load, seismic load, and wind load. In this analysis, the wind load combination case 4 (combination of dead, wind, and live loads) is employed for the sliding design of strip foundations. For foundation sliding failure, the load factors for dead, wind, and live loads are $\alpha_D = 0.9$, $\alpha_W = 1.4$, and $\alpha_L = 0.5$, respectively.

The factored design horizontal wind load, per unit foundation length, is taken to be $\alpha_W \widehat{F}_W$, where $\widehat{F}_W$ is the characteristic design wind load calculated by substituting the design wind speed, v_d, into Eq. (12) leading to the characteristic design load,

$$\hat{F}_W = (\hat{p}_{ww} - \hat{p}_{wl})H, \tag{13}$$

where $\widehat{p}_{ww}$ and $\widehat{p}_{wl}$ are the design external windward and leeward wind pressures calculated by substituting v_d into Eq. (11) and H is the building height. The design wind speed, v_d, is the 50-year return period annual maximum hourly average wind speed, and can be found for various locations from the NBC [1].

For undrained soil conditions, the sliding resistance depends on the adhesion at the interface, which is a portion of the soil undrained shear strength, αs_u, where α is the adhesion factor, ranging from 0 to 1. As the sliding failure probability is primarily governed by the variability of s_u, the value of α has a minimal effect on the resistance factor calibration. In this research, α is assumed to be 1 for simplicity, and thus the adhesion is equal to the soil undrained shear strength. The characteristic sliding resistance of strip foundations on undrained soils (cohesive) can be expressed as

$$\hat{R}_u = \hat{A}\hat{s}_u, \tag{14}$$

where $\widehat{A}$ is the foundation base area, $\widehat{A} = \widehat{B}\times 1$, with $\widehat{B}$ being the designed strip foundation width and $\hat{s}_u$ being the characteristic undrained shear strength of the soil.

The design philosophy is to determine the foundation width that minimally satisfies the LRFD inequality.

Substituting Eq. (14) into the LRFD Eq. (1) evaluated at the equality yields

$$\phi_{gu}\hat{B}\hat{s}_u - \alpha_W \hat{F}_W = 0. \tag{15}$$

The designed foundation width, $\widehat{B}$, can be obtained by solving the above equation, giving

$$\hat{B} = \frac{\alpha_W \hat{F}_W}{\phi_{gu}\hat{s}_u}. \tag{16}$$

As mentioned, the vertical live and dead loads are not involved in the sliding design of foundations on cohesive soils.

For frictional soils, the sliding resistance is only dependent on the friction angle and the vertical load and is independent of the foundation area. Considering only vertical dead and live loads, the LRFD equation becomes

$$\phi_{gu}\left[\left(\alpha_L \hat{F}_L + \alpha_D \hat{F}_D\right)\tan\hat{\phi}'\right] - \alpha_W \hat{F}_W = 0, \tag{17}$$

where ϕ_{gu} is the sliding resistance factor for frictional soils, $\widehat{\phi}'$ is the characteristic effective internal friction angle of the soil, and $\alpha_W \widehat{F}_W$ is the factored horizontal design wind load.

For a given sliding resistance factor, ϕ_{gu}, the total sliding failure probability shown by Eq. (17) can be approximated using the total probability theorem expressed as a sum of a finite number of terms,

$$p_f \approx \sum_{i=1}^{n} \boldsymbol{P}[F_W > \bar{R}_u | V = v_i] \cdot \boldsymbol{P}[V = v_i], \tag{18}$$

where v_i is a deterministic realization of the annual maximum hourly average wind speed, V; F_W is the actual horizontal wind load corresponding to v_i (assumed random), and $\bar{R}_u$ is the actual sliding resistance of the designed foundation (assumed random). The probability, $P[V = v_i]$, is obtained using the Gumbel extreme value distribution, and the conditional failure probability, $P[F_W > \bar{R}_u | V = v_i]$, is obtained using Monte Carlo simulations, with the soil having spatially random undrained shear strength or friction angle. Further details can be found in He and Fenton [40].

For cohesive soils, Figure 14 presents how sliding failure probability varies with soil spatial correlation length and resistance factor for strip foundations.

The range of the target lifetime reliability index (i.e., $\beta_m = 2.4 \rightarrow p_m = 8.2\times10^{-3}$ to $\beta_m = 3.5 \rightarrow p_m = 2.3\times10^{-4}$) for the sliding failure of shallow foundations recommended by Barker et al. [41] is also superimposed in Figure 14.

Figure 14(a) shows the failure probability for three coefficients of variation of the soil undrained shear strength as a function of the soil correlation length for $\phi_{gu} = 0.6$. The figure illustrates the existence of a "worst case" correlation length, θ. Small correlation lengths result in rapid spatial variation in the soil undrained shear strength, while large correlation lengths result in slow variation. A very small correlation length leads to reduced variance in the geometric average of the sample (i.e., characteristic undrained shear strength, $\hat{s}_u$), which results in less difference between the sample characteristic undrained shear strength, $\hat{s}_u$, and the geometric average of the undrained shear strength under the designed foundation, $\bar{s}_u$ (it is assumed here that the uncertainty in the soil property is stationary, i.e., having the same mean and standard deviation everywhere). When the correlation length is very large, the undrained shear strengths at the sample and under the designed foundation will also be very similar. Therefore, both very small and very large correlation lengths mean that for a given resistance factor the understanding of soil conditions under the foundation is high, leading to low failure probabilities. At intermediate correlation lengths, the soil sample is likely to be an imperfect estimator of the soil conditions under the foundation, so the failure probability increases. The existence of a worst case correlation has also been found in the bearing capacity design [42] and the serviceability design [43], [44] of shallow foundations. An implication for practical foundation designs is that when fewer data are available for the estimate of correlation length, the worst case correlation length can be used for conservative design.

The results in Figure 14(a) suggest that $\phi_{gu} = 0.6$, which is the resistance factor for foundation sliding on cohesive soils recommended by the CHBDC [17]. The figure shows that the estimated reliability lies mostly between $\beta_m = 2.4$ and 3.5, except a few points close to the worst case correlation length for the case of $\nu_{s_u} = 0.5$. Thus, a resistance factor of $\phi_{gu} = 0.6$ can generally be seen as a reasonable choice for foundation sliding on cohesive soils.

Figure 14(b) shows the failure probability as a function of the resistance factor for the soil spatial correlation length of $\theta = 2$ m, which is close to the worst case correlation length shown in Figure 14(a). The failure

Figure 14: Sliding failure design of strip foundations on cohesive soils showing the failure probability for three coefficients of variation of the soil undrained shear strength as a function of the soil correlation length for ϕ_{gu} = 0.6 in (a); and the failure probability as a function of the resistance factor for θ = 2 in (b).

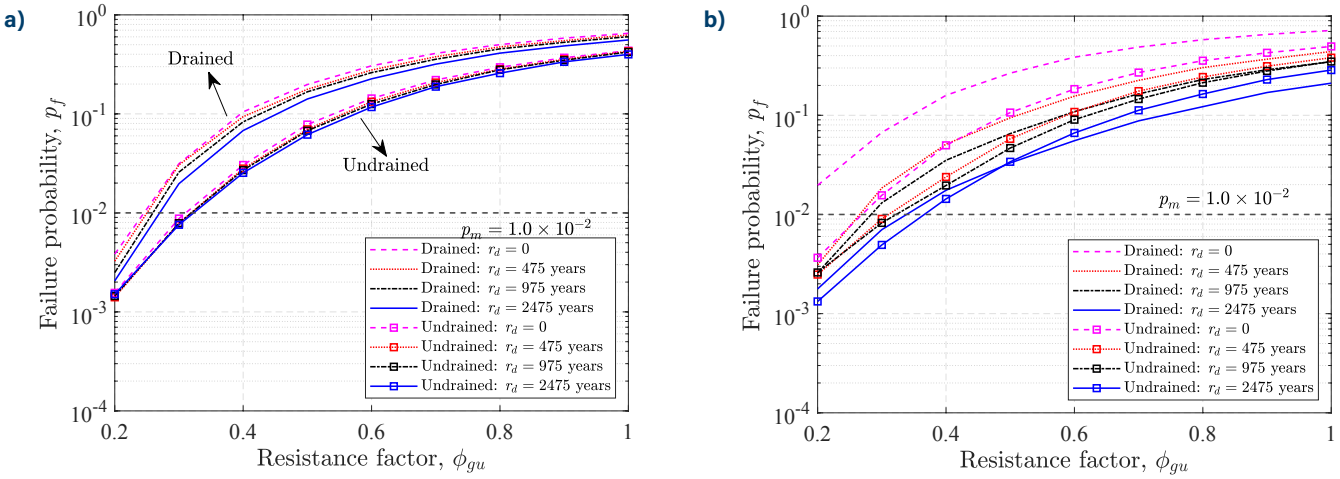

probability increases with the resistance factor, as expected. Assuming moderate soil variability (i.e., $\nu_{s_u} = 0.3$), the required resistance factor is ranges from 0.4 to 0.65, so the $\phi_{gu} = 0.6$ prescribed by the CHBDC [17] seems to be appropriate.

Figure 15 illustrates the sliding failure probability of strip foundations on frictional soils for four coefficients of variation of the soil effective internal friction angle as a function of the resistance factor. The range of the target lifetime reliability index shown in Figure 14 is also incorporated in Figure 15 for comparison. The figure shows that the curves for different values of $\nu_{\phi'}$ fall into a narrow band, indicating that the values of $\nu_{\phi'}$ of practical interest have a relatively minor influence on the sliding failure probability. Compared to the target maximum failure probability, the required resistance factor for $\nu_{\phi'}$ = 0.15 is ranges from 0.5 to 0.85. The resistance factor for foundation sliding on frictional soils recommended by the CHBDC [17] is 0.8. As shown in Figure 15, the failure probabilities at $\phi_{gu} = 0.8$ for all the values of $\nu_{\phi'}$ lie in the range of the target maximum failure probability. Therefore, it appears that the resistance factor recommended by the CHBDC [17] is also reasonable for the sliding design of shallow foundations for buildings.

Figure 15: Sliding failure design of strip foundations on frictional soils showing the failure probability for four coefficients of variation of the soil effective internal friction angle as a function of the resistance factor.

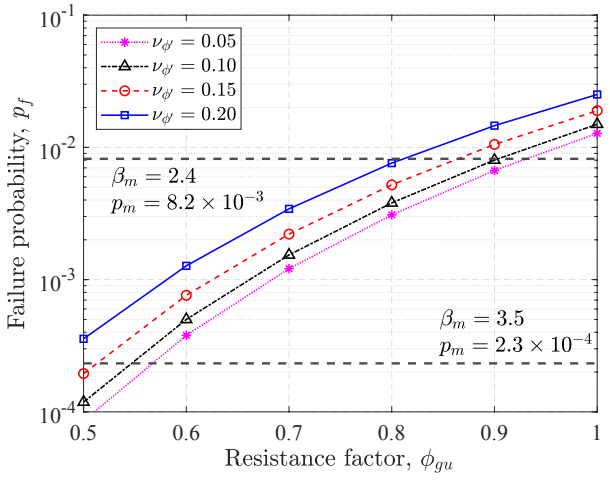

In summary, Monte Carlo simulations were used to investigate the sliding resistance of cohesive soils. The designed foundation width was first evaluated using the LRFD method and then Monte Carlo simulations were performed to estimate the sliding failure probability of the designed foundation. However, frictional soils were studied analytically because the sliding resistance of a shallow foundation on frictional soils is determined only by the vertical load on the foundation and the effective internal friction angle of the soil under the foundation, and is not affected by the foundation dimension. Parametric analyses were carried out by varying ν_{s_u} for cohesive soils and $\nu_{\phi'}$ for frictional soils. For both cases, the geotechnical sliding resistance factors required to achieve the target lifetime failure probability were estimated.

For cohesive soils, the results indicate the existence of a worst case correlation length, which has also been found in the bearing resistance design and serviceability design of shallow foundations by other researchers. The required resistance factor ranges from 0.4 to 0.65 for an intermediate value of $\nu_{s_u} = 0.3$, so the choice of $\phi_{gu} = 0.6$ recommended by the CHBDC [17] appears to be reasonable. For frictional soils, the practical range of $\nu_{\phi'}$ considered in this analysis has a limited effect on the sliding failure probability. The required resistance factor for $\nu_{\phi'} = 0.15$ ranges from 0.5 to 0.85, which is in agreement with the CHBDC [17] recommendation of $\phi_{gu} = 0.8$ for frictional soils.

It should be emphasized that the resistance factors recommended here are conservative for several reasons. For one thing, the actual correlation length of the soil is unlikely to equal the worst case value. Furthermore, in practice, foundations of buildings are generally embedded in the ground rather than lying on the surface. However, the results are also unconservative for other reasons. For example, this analysis did not consider measurement and model errors. To some extent, these conservative and unconservative factors cancel each other out, and the agreement between the results discussed in this research and the code recommendations suggest that this analysis is reasonably accurate.

8 Sliding and Overturning of Retaining Walls

In this section, the resistance factors required to design a retaining wall against sliding and overturning at a certain reliability level are estimated. The primary retained soil parameters, which affect the design of gravity retaining walls, are the unit weight, γ_s, and the effective internal friction angle, ϕ', of the soil, which are represented by two spatially random fields and characterized by their means, standard deviations, and correlation lengths.

The soil unit weight is assumed to be lognormally distributed because the lognormal distribution is strictly non-negative and has a simple relationship with the normal distribution. Following Fenton and Griffiths [11], the effective internal friction angle field is assumed to be bounded between 20° and 40° (having a mean of $\mu_{\phi'} = 30^\circ$) following a marginal tanh distribution with a scale parameter of $s = 3$. The scale parameter governs the effective internal friction angle variability between the two bounds and $s = 3$ corresponds to a standard deviation of $\sigma_{\phi'} \simeq 4^\circ$ (i.e., a coefficient of variation of $\nu_{\phi'} = \frac{\sigma_{\phi'}}{\mu_{\phi'}} \simeq 0.13$). The value of $\nu_{\phi'} \simeq 0.13$ is consistent with the coefficient of variation range of practical interest (i.e., $0.1 \leq \nu_{\phi'} \leq 0.2$. The correlation structure of both soil properties is assumed to be Markovian. Further details of this research are available in He *et al.* [45].

Figure 16 shows a diagram of the gravity retaining wall system. For simplicity, the retaining wall is depicted as a rectangular block; the important factors are its weight and footprint.

Based on Rankine's theory, the characteristic design lateral active earth load, $\widehat{F}_a$, and overturning moment, $\widehat{M}_a$, acting on the gravity retaining wall can be expressed by Eq. (19) with the hat parameters used for retaining wall design:

$$\widehat{F}_a = \frac{1}{2}\widehat{\gamma}_s H^2 \widehat{K}_a, \tag{19a}$$

$$\widehat{M}_a = \frac{1}{3}\widehat{F}_a H = \frac{1}{6}\widehat{\gamma}_s H^3 \widehat{K}_a, \tag{19b}$$

where $\widehat{\gamma}_s$ is the characteristic unit weight; H is the wall height, which is held constant in this analysis; and $\widehat{K}_a$ is the characteristic active earth pressure coefficient, which is given by

$$\widehat{K}_a = \tan^2\left(45^\circ - \frac{\widehat{\phi}'}{2}\right), \tag{20}$$

where $\widehat{\phi}'$ is the characteristic effective internal friction angle, in degrees. As demonstrated by Kim [46], the retaining wall height (deterministic) has a negligible effect on the failure probabilities for sliding and overturning limit states.

Figure 16: Schematic of a gravity retaining wall with soil sampling location shown.

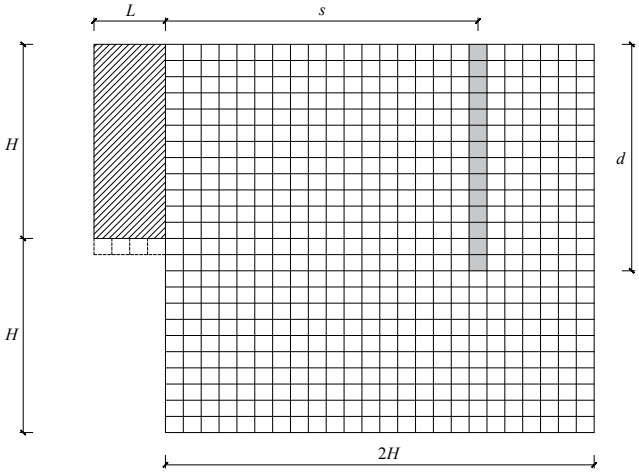

The characteristic sliding resistance of the designed gravity retaining wall is estimated to be the friction at the soil-wall base interface,

$$\widehat{R}_s = \gamma_w H \widehat{L} \tan\widehat{\phi}', \tag{21a}$$

where γ_w is the unit weight of the wall (assumed deterministic) and $\widehat{L}$ is the designed wall width. The characteristic overturning resistance of the designed wall is contributed purely by the wall self-weight about the toe (bottom-left point) of the wall,

$$\widehat{R}_o = \frac{1}{2}\gamma_w H \widehat{L}^2. \tag{21b}$$

Note that the overturning resistance is determined only by the wall itself and the soil is not involved. In this research, the wall height, H, is held constant and

the design philosophy is to estimate the wall width that satisfies the LRFD inequality. Substituting the characteristic loads, Eq. (19), and the characteristic resistances, Eq. (21), into Eq. (1) yields the following LRFD equations for sliding and overturning limit states:

$$\phi_{gu}\left(\gamma_w H\hat{L}\tan\hat{\phi}'\right)-\frac{1}{2}\alpha_E\hat{\gamma}_s H^2\hat{K}_a=0 \qquad (22a)$$

for sliding mode, and

$$\phi_{gu}\left(\frac{1}{2}\gamma_w H\hat{L}^2\right)-\frac{1}{6}\alpha_E\hat{\gamma}_s H^3\hat{K}_a=0 \qquad (22b)$$

for overturning mode.

The designed wall base widths, $\widehat{L}$, for sliding and overturning limit states can then be estimated by solving the above LRFD equations for $\widehat{L}$, giving

$$\hat{L}=\frac{\alpha_E\hat{\gamma}_s\hat{K}_a}{2\phi_{gu}\gamma_w\tan\hat{\phi}'} \qquad (23a)$$

for sliding mode, and

$$\hat{L}=\sqrt{\frac{\alpha_E\hat{\gamma}_s\hat{K}_a}{3\phi_{gu}\gamma_w}}\cdot H \qquad (23b)$$

for overturning mode.

Once the actual resistances and loads are determined, the designed retaining wall can be checked to see whether or not the design is safe. Monte Carlo simulations are used to estimate the probabilities of failure. For a given resistance factor, ϕ_{gu}, the detailed steps of the simulation are:

1. Using the LAS method, simulate the random fields of the soil properties, γ_s and ϕ', having the specified means, standard deviations, and correlation lengths.
2. Virtually sample the soil at a distance, s, from the retaining wall and calculate the characteristic soil parameters, $\widehat{\gamma}_s$ and $\widehat{\phi}'$.
3. Design the retaining wall to obtain the designed wall base width, $\widehat{L}$, for the given resistance factor, ϕ_{gu}, using Eq. (23) for both sliding and overturning limit states.
4. Construct the finite element model based on the designed wall base width and estimate the actual sliding and overturing loads.
5. Compute the actual sliding and overturning resistances and determine whether the designed retaining walls fail regarding sliding and overturning limit states.
6. Repeat steps 1 to 5 multiple times (n_{sim}) and record the number of failures (n_{fail}). The failure probability of the designed retaining wall is then estimated to be $p_f \approx \frac{n_{fail}}{n_{sim}}$.

Note that for each realization of the random fields, the design and subsequent failure probability evaluation of the gravity retaining wall are performed separately for sliding and overturning limit states. The entire process above is repeated for different resistance factors to estimate the failure probabilities as a function of the resistance factor.

To determine resistance factors required to achieve given target reliabilities, the target lifetime failure probabilities, p_m, should be established. The values of p_m, for different limit states (i.e., failure modes) are generally different. Therefore, the target failure probabilities for sliding and overturning limit states of gravity retaining walls should be separately given. However, separate target values of p_m, for sliding and overturning limit states are rarely seen in the literature. This research uses the failure probability ranges derived by Kim [46], using a first order second moment method. The soil unit weight, γ_s, internal friction angle, ϕ', and wall unit weight, γ_w, are considered to be random variables. Parametric analyses performed by Kim [46] show that the ranges of the sliding and overturning failure probabilities are 0.71×10^{-2} to 4.35×10^{-2} and 0.20×10^{-4} to 25.4×10^{-4} respectively.

Figure 17 presents the failure probabilities of the gravity retaining walls for sliding and overturning limit states as a function of the resistance factor, ϕ_{gu}. Note that for the overturning limit state, a total number of realizations of $n_{sim}=10000$ is unable to assess the failure probability, p_f, at $\phi_{gu}=0.5$ because p_f is less than 10^{-4}. In this analysis, the overturning p_f at $\phi_{gu}=0.5$ is extrapolated using a quadratic polynomial fit to the probabilities estimated by RFEM for ϕ_{gu} = 0.6 to 1.0.

Figure 17 shows that the failure probability for the sliding mode is consistently greater than that for the overturning mode, particularly for lower values of ϕ_{gu}. This is primarily due to the larger variability in the actual sliding resistance than in the actual overturning resistance. Eq. (21a) indicates that once the wall is

designed, the actual sliding resistance, $\bar{R}_s$, depends on the spatially variable soil, while the actual overturning resistance, $\bar{R}_o$, depends only on the deterministic wall properties. For ϕ_{gu} ranging from 0.5 to 1.0, the sliding failure probability varies from 5.4×10^{-3} to 2.3×10^{-1}, and the overturning failure probability ranges from 1.5×10^{-5} to 1.8×10^{-1}. The comparison between the failure probabilities for the two limit states suggests that the overturning failure probability is much more sensitive to the resistance factor than is the sliding failure probability.

Figure 17: Gravity retaining wall design results showing the failure probabilities for sliding and overturning limit states.

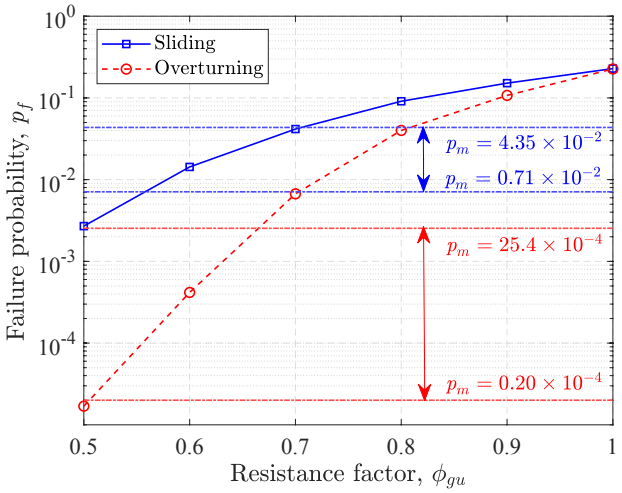

Compared to the target sliding failure probability ($p_m = 1.58\times10^{-2}$), the required resistance factor for the sliding limit state is ranges from 0.52to 0.68, which is lower than $\phi_{gu} = 0.8$ recommended by the CHBDC [17]. The value of $\phi_{gu} = 0.8$ corresponds to a failure probability of $p_f = 0.1$, which is relatively high. Fenton *et al.* [44] showed that it is conservative to take the soil unit weight and effective internal friction angle to be independent (the case considered in this research). However, the resistance factors for the sliding limit state based on a strong correlation between the soil unit weight and effective internal friction angle are more consistent with the CFEM [2]. In practice, the soil unit weight and effective internal friction angle generally have a significant positive correlation [47], [48], so the value of $\phi_{gu} = 0.8$ may still be a reasonable choice.

For the overturning limit state, the required resistance factor to achieve the target failure probability is ranges from 0.51 to 0.68, which is almost the same as the resistance factor range for the sliding limit state. The value of $\phi_{gu} = 0.5$ prescribed by the CHBDC [17] seems to be acceptable and relatively conservative.

9 Reliability-Based Design Versus Load and Resistance Factor Design

The LRFD approach used in many geotechnical design codes is often calibrated using the reliability-based design (RBD) method. However, the LRFD may not be able to precisely achieve the target safety level. In the RBD approach, the design parameters are treated as random variables or fields and the probability of failure is estimated based on the distributions of the loads and ground properties. In this research, the RFEM (specifically, the custom programs "rbear2d" and "rsetl2d") is used to estimate the bearing capacity and settlement failure probabilities of strip foundations. The finite element models are derived from Smith et al. [21].

Monte Carlo simulations are performed for the analysis, modeling the soil as a spatially varying random field. Random maximum lifetime loads are then applied to the geotechnical system, in this case a strip foundation, and a finite element analysis is used to check whether the particular limit state under consideration is exceeded. The soil properties (e.g., undrained shear strength, s_u, for ULS; and elastic modulus, E, for SLS) are assumed to follow non-negative distributions, having specified means, standard deviations, and spatial correlation lengths. The live and dead loads are assumed to be lognormally distributed. Further details of the random soil and load models are discussed below (also, see Fenton et al. [42] for ULS and Fenton et al. [44] for SLS). The detailed steps of the RFEM used in this section are:

1. For a particular limit state (i.e., ULS or SLS), choose a strip foundation width to be used in the finite element model.
2. Simulate the random fields of the soil properties (i.e., s_u for ULS; and E for SLS), having the specified means, standard deviations, and spatial correlation lengths.

3. Place a foundation with the width prescribed in step 1 on the simulated random fields in the finite element model; simulate live and dead loads and apply them to the foundation centre.
4. Use the finite element method to determine if the foundation enters (fails) the particular limit state under consideration.
5. Repeat steps 2 to 4 n_{sim} times, and record the number of failures (n_{fail}). The failure probability of the strip foundation with the width prescribed in step 1 is then estimated as $p_f \approx \frac{n_{fail}}{n_{sim}}$.

The entire process is repeated for various foundation widths to estimate the failure probability as a function of foundation width.

Sections 9.1 to 9.4 discuss the ULS and SLS design of strip foundations within the LRFD framework.

9.1 Ultimate Limit State

For simplicity, this research considers surface strip foundations on cohesive soils under undrained soil conditions. The bearing capacity equation for surface strip foundations subjected to vertical loading, without surcharge, is given by the CHBDC [17], with the hat parameters used for foundation design, as

$$\hat{q}_u = \hat{s}_u N_c, \tag{24}$$

where $\hat{q}_u$ is the characteristic ultimate bearing resistance (in units of pressure), $\hat{s}_u$ is the characteristic soil undrained shear strength, and N_c is the bearing capacity factor (i.e., $N_c = \pi + 2$) for undrained soil conditions.

The characteristic ultimate resistance of the designed strip foundation, in units of force, is estimated as

$$\hat{R}_u = \hat{B}\hat{q}_u = \hat{s}_u N_c \hat{B}, \tag{25}$$

where $\hat{B}$ is the designed foundation width. The LRFD philosophy is to estimate the foundation width that satisfies the inequality in Eq. (1). Substituting Eq. (25) into Eq. (1) for ULS yields, at the equality,

$$\phi_{gu}\hat{s}_u N_c \hat{B} - \alpha_{Tu}\hat{F}_{Tu} = 0. \tag{26}$$

The required foundation width, $\hat{B}$, is then estimated by solving the above equation for $\hat{B}$, giving

$$\hat{B} = \frac{\alpha_{Tu}\hat{F}_{Tu}}{\phi_{gu}\hat{s}_u N_c}. \tag{27}$$

Note that the characteristic soil undrained shear strength, $\hat{s}_u$, is taken here as its corresponding mean, μ_{s_u}.

9.2 Serviceability Limit State

In this research, the foundation is assumed to be rigid and a finite supporting soil layer (having thickness h) is considered, as shown in Figure 18. The LRFD design goal is to determine the foundation width, $\hat{B}$, such that the predicted settlement does not exceed a specified tolerable settlement, δ_{max}. Rowe and Booker [49] found that the settlement of a rigid strip foundation under a vertical load can be assumed to be 84% of the central settlement of a flexible foundation. For a homogeneous soil layer, the ratio of rigid settlement to central flexible settlement is dependent on the ratio, $\frac{h}{b}$ and the value of 0.84 is the average of many cases [49]. According to the CFEM [2], the characteristic serviceability resistance of a flexible strip foundation resting on the surface of a uniform layer of isotropic elastic soil is calculated using the following equation, with the hat parameters used for foundation design:

$$\hat{R}_S = \hat{q}\hat{B} = \frac{\delta_{max}\hat{E}}{\hat{I}_s}, \tag{28}$$

where $\hat{R}_s$ is the characteristic serviceability resistance, δ_{max} is a specified tolerable settlement, $\hat{q}$ is the average pressure applied to the ground by the foundation at a settlement equal to δ_{max}, $\hat{E}$ is the characteristic elastic modulus of the soil, and $\hat{I}_s$ is an influence factor, which is a function of the soil Poisson's ratio, ν, and the ratio of the soil layer depth to the designed foundation width, $\frac{h}{b}$.

The settlement of a rigid strip foundation is estimated by applying the ratio of 0.84 to Eq. (28),

$$\hat{R}_S = \frac{\delta_{max}\hat{E}}{0.84\hat{I}_s}. \tag{29}$$

The influence factor, $\hat{I}_s$, is a function of ν and $\frac{h}{\hat{B}}$. For ν = 0.3, the relationship between $\hat{I}_s$ and $\frac{h}{\hat{B}}$ given by the CFEM [2] is closely approximated by a power function obtained using the MATLAB Curve Fitting Toolbox®,

$$\hat{I}_s = 8.85\left(\frac{h}{\hat{B}}\right)^{0.06} - 8.16. \quad (30)$$

Substituting Eq. (29) into the LRFD Eq. (1) gives

$$\phi_{gs}\frac{\delta_{max}\hat{E}}{0.84\hat{I}_s} \geq \alpha_{Ts}\hat{F}_{Ts}. \quad (31)$$

The designed foundation width, $\hat{B}$, required for SLS is then estimated by solving Eq. (31) at the equality using Eq. (30) to give

$$\hat{B} = H \cdot \left(0.113\phi_{gs} \cdot \frac{\delta_{max}\hat{E}}{0.84\alpha_{Ts}\hat{F}_{Ts}} + 0.922\right)^{-1/0.06}. \quad (32)$$

Similar to ULS, the characteristic soil elastic modulus, $\hat{E}$, is taken as its mean, μ_E.

Figure 18: Schematic foundation and soil layer.

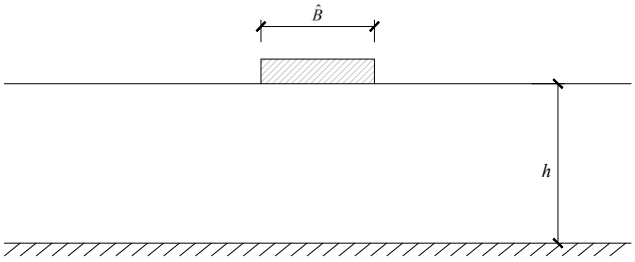

For this research, a five-storey office building (6 m wide and 5 × 3 m in height) supported by two strip foundations is used as an example. Only the vertical loads acting on the foundation induced by live and dead loads from the building are considered. The live load acting on each floor is obtained from the NBC [1] and the dead load is taken as three times the live load [32]. The coefficients of variation of dead and live loads are assumed to be $\nu_D = 0.15$ [5] and $\nu_L = 0.3$ [6], [7], respectively. Following the load combination case 2 for ULS prescribed by the NBC [1], the live and dead load factors for ULS are $\alpha_{Lu} = 1.5$ and $\alpha_{Du} = 1.25$, while the live and dead load factors for SLS are 1.0 (i.e., $\alpha_{Ls} = 1.0$ and $\alpha_{Ds} = 1.0$).

Table 3 summarizes the parameters used for the LRFD and RBD designs. In RBD, the random fields are s_u for ULS and E for SLS, and the dead and live loads are assumed to be random and lognormally distributed. For ULS, the soil undrained shear strength, s_u, is assumed to be lognormally distributed, having a mean of $\mu_{s_u} = 100$ kPa and a coefficient of variation of $\nu_{s_u} = 0.3$ (i.e., standard deviation of $\sigma_{s_u} = 30$ kPa), which is consistent with the range of $\nu_{s_u} = 0.2$ to 0.5 recommended by Lee et al. [36]. For SLS, the soil elastic modulus, E, has a mean of $\mu_E = 10$ MPa and is assumed to be lognormally distributed. The coefficient of variation of the soil elastic modulus, ν_E, reported by Lee et al. [36] is 0.02 to 0.42. Values of $\nu_E = 0.1$, 0.2, and 0.3 (i.e., $\sigma_E = 1$, 2 and 3 MPa) are used in this research. Various spatial correlation lengths of the random field soil properties (i.e., for s_u and E, and assumed equal) are considered as θ = 0.1, 0.5, 1.0, 2.0, 5.0, 10.0, 20.0, and 50.0 m.

Table 3: Input Parameters for Load and Resistance Factor Design and Reliability-Based Design

Parameters	Values
Soil undrained shear strength: μ_{s_u}, σ_{s_u}(kPa)	100; 30 (ν_{s_u} = 0.3)
Soil elastic modulus: μ_E, σ_E (MPa)	10; 1, 2, 3 (ν_E = 0.1, 0.2, 0.3)
Live load: μ_L, σ_L (kN/m)	43.9; 13.2 (ν_L = 0.3)
Dead load: μ_D, σ_D (kN/m)	131.7; 19.8 (ν_D = 0.15)
Load factors (ULS): α_{Lu}, α_{Du}	1.5; 1.25
Load factors (SLS): α_{Ls}, α_{Ds}	1.0; 1.0
Resistance factor (ULS): ϕ_{gu}	0.5
Resistance factor (SLS): ϕ_{gs}	1.0, 0.8, 0.7, 0.65
Spatial correlation length: θ (m)	0.1, 0.5, 1.0, 2.0, 5.0, 10.0, 20.0, 50.0
Thickness of soil layer: h (m)	6.4
Soil Poisson's ratio: ν	0.3
Number of realizations: n_{sim}	10 000

The thickness of the soil layer is taken to be $h = 6.4$ m and the soil Poisson's ratio is assumed to be 0.3. Following the NBC User's Guide [8], a resistance factor of $\phi_{gu} = 0.5$ is employed for the ULS bearing resistance design of shallow foundations. The CFEM [2] suggests $\phi_{gs} = 1.0$ for the settlement design of shallow foundations, but the CHBDC [17] recommends $\phi_{gs} = 0.8$. In this research, values of ϕ_{gs} ranging from 0.65 to 1.0 are investigated. The maximum tolerable settlement, δ_{max}, is taken to be 0.025 m, as recommended by the NBC User's Guide [8], and a total number of $n_{sim} = 10000$ realizations are used in the RBD Monte Carlo simulations. As mentioned above, the characteristic values, $\hat{s}_u$ and $\widehat{E}$, used in the LRFD approach are assumed to be their corresponding means, μ_{s_u} and μ_E, respectively.

9.3 Ultimate Limit State Design Results

Figure 19 shows how failure probability varies with the designed foundation width and spatial correlation length, as obtained by the RBD method for ULS. The range of the target lifetime reliability index (i.e., $\beta_m = 2.8 \rightarrow p_m = 2.56\times10^{-3}$ to $\beta_m = 3.5 \rightarrow p_m = 2.33\times10^{-4}$) for shallow foundations recommended by Becker [6], [7] for the NBC [1] is also superimposed in Figure 19a. The LRFD designed foundation width is $\widehat{B} = 0.88$ m (see the black vertical line in Figure 19a).

As shown in Figure 19a, the failure probability decreases with increased foundation width, as expected. The failure probability is also dependent on the spatial correlation length of the soil, θ, particularly

Figure 19: ULS design results showing the probability of failure (a), the RBD required foundation width for $p_m = 2.56\times10^{-3}$ (b), and the failure probability, p_f, for two foundations widths as a function of the correlation length (c).

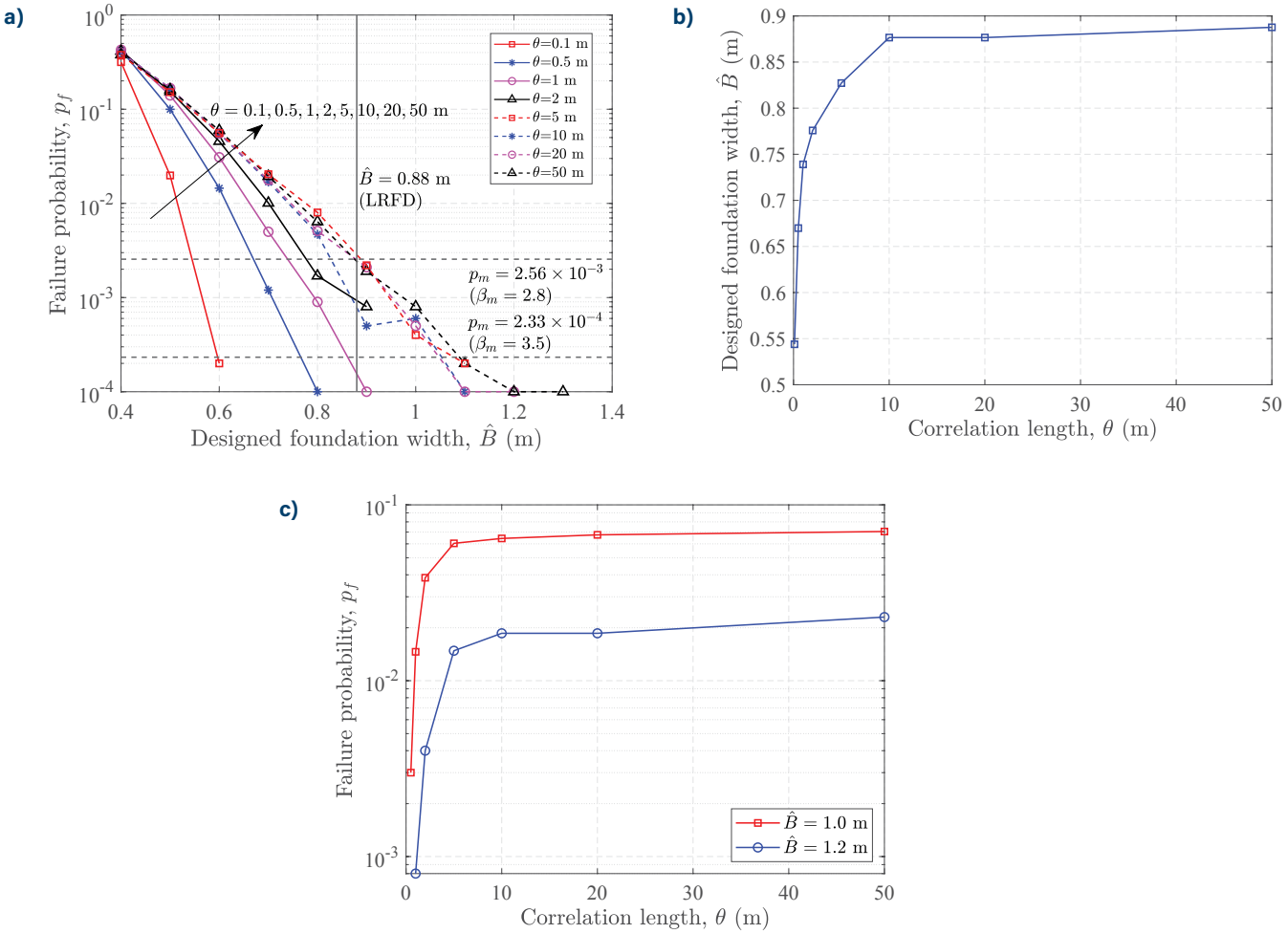

for smaller values of θ. The figure can be used for foundation design by drawing a horizontal line at the maximum acceptable failure probability, p_m, (which would commonly be between $p_m = 2.33\times10^{-4}$ and 2.56×10^{-3}) and reading off he required foundation width for a given θ. For example, if $p_m = 2.56\times10^{-3}$) (i.e., $\beta m = 2.8$) is desired, then Figure 19b shows the required foundation width as a function of the spatial correlation length. Figure 19b suggests that the designed foundation width shows an approximately linear increase with θ for relatively small values of $\theta(\theta \leq 2m)$, and then gradually approaches a plateau (close to $\widehat{B} = 0.88$ m for this case of $p_m = 2.56\times10^{3}$).

9.4 Serviceability Limit State Design Results

According to the LRFD approach, for ϕ_{gs} = 1.0, the designed foundation width for SLS is $\widehat{B} = 1.0$ m.

Similarly, the LRFD gives designed foundation widths, $\widehat{B} = 1.81$, 2.46, and 2.87 m, for $\phi_{gs} = 0.8$, 0.7, and 0.65, respectively.

Figure 20 presents the failure probabilities of the SLS design estimated by the RBD method for eight values of θ and three values of ν_E. In contrast to the ULS results in Figure 19a, the failure probability for SLS appears to be less dependent on the soil correlation length, particularly for smaller foundation widths. For larger foundation widths ($\widehat{B} > 2$ m), Figure 20 suggests that the dependence of p_f on θ gradually increases with increasing coefficient of variation of E, ν_E.

The maximum acceptable lifetime failure probabilities, 10^{-1} to 10^{-3}, for SLS are also superimposed in Figure 20. If the failure probability range is assumed reasonable, then Figure 20 suggests that the LRFD approach with $\phi_{gs} = 1.0$ ($\widehat{B} = 1.00$ m) is unconservative when

Figure 20: SLS design results showing the failure probabilities for ν_E = 0.1 (a); ν_E = 0.2 (b); and ν_E = 0.3 (c).

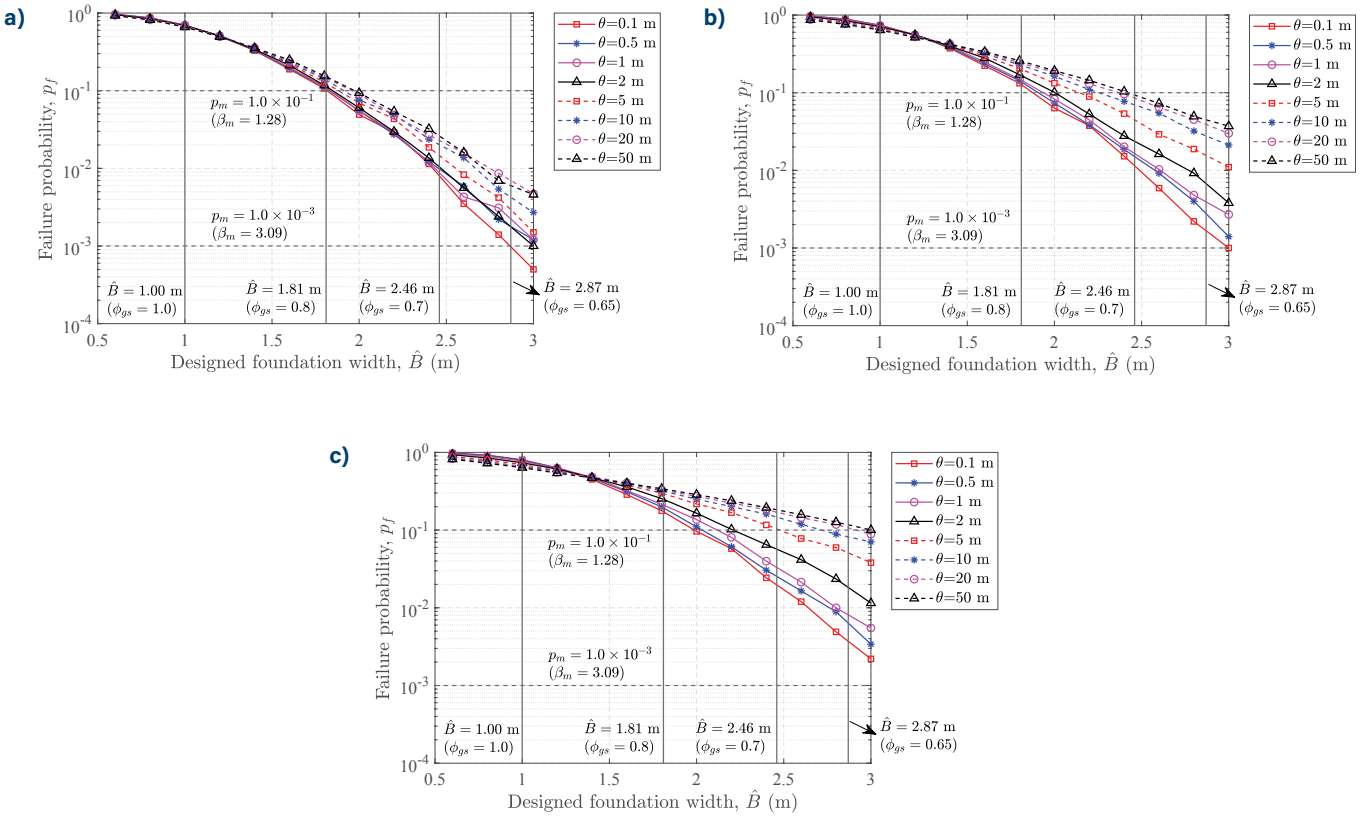

compared to the RBD method. Note that for any correlation length, the RBD approach suggests a failure probability (i.e., the probability that the ground resistance at $\delta_{max} = 0.025$ m is less than the applied load) of about 0.7. For correlation lengths less than 2 m ($\theta \leq 2$ m), resistance factors ranging from 0.65 to 0.8 provide failure probabilities ranging from approximately 1×10^{-3} to 1×10^{-1}. Thus, the recommendation of ϕ_{gs} = 0.8 by the CHBDC [17] seems reasonable. However, if p_m is taken to be 10^{-2}, then ϕ_{gs} = 0.65 to 0.7 seems more appropriate for $\theta \leq 2$ m.

10 Summary

This research summarizes the results from a study on target reliability levels for geotechnical systems and the resistance factors required to achieve the targets within the LRFD framework, and from a study on direct RBD as an alternative to the LRFD approach. The major findings are:

1. In North America, target lifetime reliabilities of non-redundant geotechnical systems at ULS are around $\beta = 3.0$, corresponding to a target maximum acceptable failure probability of around $p_m = 1/1000$. The results suggest that this target is not always met and that sometimes the actual reliability achieved for ULS design is as low as 2.5. However, the ULS target reliability index of 3.0 can be reduced to $\beta = 2.0$ to 2.5 (target failure probability ranging from $p_m = 0.006$ to 0.020) if the geotechnical system has redundancy. For SLS design, Fenton et al. [14] suggested a failure probability of about ten times that for ULS. In other words, if $p_m = 1/1000$ ($\beta = 3.0$) for ULS, then $p_m = 1/100$ ($\beta = 2.3$) would be acceptable for SLS. In practice, actual reliability levels for SLS design as high as $p_m = 4/100$ ($\beta = 1.8$) are suggested. The results suggest that lifetime reliability targets of $p_m = 1/1000$ ($\beta = 3.0$) should be adopted for ULS design of non-redundant systems, while for redundant systems, these targets can be relaxed to $p_m = 1/100$ ($\beta = 2.3$). Similarly, for SLS, the target lifetime reliability can be $p_m = 1/100$ ($\beta = 2.3$) for non-redundant systems and $p_m = 4/100$ ($\beta = 1.8$) for redundant systems. For buildings, the effect of failure consequence severity on target failure probability has yet to be investigated.

2. For seismic design, target lifetime failure probabilities are more complicated to define because increasing damage for higher magnitude earthquakes is deemed to be acceptable. This means that the target lifetime failure probability changes as a function of what magnitude earthquakes occur during the design lifetime. The resulting specification of target geotechnical reliabilities for seismic design was therefore beyond the scope of this research. For the purposes of this research, static reliability index targets of $\beta = 1.8$ to 3.0 were investigated.

3. For seismic geotechnical design of piles, the resistance factors for seismic design suggested by the current code were found to be unconservative, failing to achieve target reliabilities. The results demonstrate that the use of static resistance factors (e.g., $\phi_{gu} = 0.4$ instead of $\phi_{gu} = 1.0$) yields reliabilities much closer to the targets.

4. For shallow foundations designed at ULS under wind and seismic loading, the resistance factors required to achieve even $p_m = 1/100$ ($\beta = 2.3$) were below $\phi_{gu} = 0.4$, and often significantly below. This may be because for load combinations 4 and 5 of the NBC [1], the live and dead load factors are reduced so all of the safety requirements are thrown onto the single resistance factor. The overall set of load combinations may need further review for geotechnical applications.

5. Geotechnical resistance factors required for the ULS sliding resistance design of shallow foundations for buildings recommended by the NBC [1] appear to be in agreement with the values recommended by the CHBDC [17].

6. Resistance factors required for the design of retaining walls against sliding ranged from 0.5 to 0.7, which is lower than that currently recommended by the CHBDC ($\phi_{gu} = 0.8$) [17]. Conversely, resistance factors required to design a retaining wall against overturning had the same range (0.5 to 0.7), which is somewhat higher than that currently recommended by the CHBDC ($\phi_{gu} = 0.5$) [17].

"In general, the results indicate that the geotechnical resistance factors for buildings are in the same range as those suggested by the CFEM and the NBC User's Guide for static design conditions."

7. The alternative RBD approach suggested potential financial savings while providing at least the same safety levels, if not higher. Further research into this alternative design approach is needed, particularly in different areas, such as slope design.

In general, the results indicate that the geotechnical resistance factors for buildings are in the same range as those suggested by the CFEM and the NBC User's Guide for static design conditions. However, the results also indicate that all of the seismic design geotechnical resistance factors are lower than — and sometimes significantly lower than — what is currently suggested in practice for buildings and bridges in Canada. There are three possible reasons for this, which will be investigated in the future:

1. The target reliability of geotechnical systems supporting buildings under extreme loading events is not clearly defined. As previously mentioned, higher levels of damage are accepted for higher magnitude earthquakes.
2. The load combinations specified by the NBC for earthquake and wind loading provide no safety contribution in the dead, live, and snow loading components to the design equation. Consequently, the entire responsibility for safety rests on the single resistance factor, which forces it to be lower because the dead, live, and snow loads are random.
3. The actual distributions of dead, live, and snow loads that might be present during short duration extreme loads (earthquake and wind) are still unknown, making estimates of failure probability under extreme loads difficult.

Other areas that require additional research for the calibration of geotechnical resistance factors include: 1) resistance factors for anchor design, 2) LRFD versus RBD design of embankments, and 3) effects of differing failure consequences on target reliabilities.

References

[1] *National Building Code of Canada,* 14th ed., NBC 2015, National Research Council of Canada, Ottawa, Canada, 2015, https://doi.org/10.4224/40002005.

[2] Canadian Geotechnical Society, *Canadian Foundation Engineering Manual,* 4th ed., Richmond, Canada, 2006.

[3] *Eurocode 7: Geotechnical Design,* EN 1997, European Committee for Standardization (CEN), Brussels, Belgium, 2004.

[4] D.E. Allen, "Limit states design—a probabilistic study," *Can. J. Civ. Eng.,* vol. 2, no. 1, pp. 36–49, 1975, https://doi.org/10.1139/l75-004.

[5] F.M. Bartlett, H.P. Hong, and W. Zhou, "Load factor calibration for the proposed 2005 edition of the National Building Code of Canada: Statistics of loads and load effects," *Can. J. Civ. Eng.,* vol. 30, no. 2, pp. 429–439, 2003, https://doi.org/10.1139/l02-087.

[6] D.E. Becker, "Eighteenth Canadian geotechnical colloquium: Limit states design for foundations. Part I. An overview of the foundation design process," *Can. Geotech. J.,* vol. 33, no. 6, pp. 956–983, 1997, https://doi.org/10.1139/t96-124.

[7] D.E. Becker, "Eighteenth Canadian geotechnical colloquium: Limit states design for foundations. Part II. Development for the national building code of Canada," *Can. Geotech. J.,* vol. 33, no. 6, pp. 984–1007, 1997, https://doi.org/10.1139/t96-125.

[8] National Research Council of Canada, Structural Commentaries *(User's Guide: NBC 2015: Part 4 of Division B),* Ottawa, Canada, 2015, https://doi.org/10.4224/40002023.

[9] G.A. Fenton and D.V. Griffiths, "Statistics of block conductivity through a simple bounded stochastic medium," *Water Resour. Res.,* vol. 29, no. 6, pp. 1825–1830, 1993, https://doi.org/10.1029/93WR00412.

[10] D.V. Griffiths and G.A. Fenton, "Seepage beneath water retaining structures founded on spatially random soil," *Géotechnique,* vol. 43, no. 4, pp. 577–587, 1993, https://doi.org/10.1680/geot.1993.43.4.577.

[11] G.A. Fenton and D.V. Griffiths, *Risk Assessment in Geotechnical Engineering.* New York, NY, USA: John Wiley & Sons, 2008.

[12] G.A. Fenton and D.V. Griffiths, "Bearing-capacity prediction of spatially random c-ϕ soils," *Can. Geotech. J.,* vol. 40, no. 1, pp. 54–65, 2003, https://doi.org/10.1139/t02-086.

[13] G.A. Fenton and E.H. Vanmarcke, "Simulation of random fields via local average subdivision," *J. Eng. Mech.,* vol. 116, no. 8, pp. 1733–1749, 1990, https://doi.org/10.1061/(ASCE)0733-9399(1990)116:8(1733).

[14] G.A. Fenton, F. Naghibi, D. Dundas, R.J. Bathurst, and D.V. Griffiths, "Reliability-based geotechnical design in 2014 Canadian highway bridge design code," *Can. Geotech. J.,* vol. 53, no. 2, pp. 236–251, 2016, https://doi.org/10.1139/cgj-2015-0158.

[15] G. Esposito and G.A. Fenton, "Review of reliability levels achieved by geotechnical design codes," presented at the 71st Can. *Geotech. Conf. (GeoEdmonton 2018),* Edmonton, Canada, Sep 23–26, 2018, Paper no. 416.

[16] *Earth-Retaining Structures,* AS 4678–2002, Standards Australia, Sydney, Australia, 2002.

[17] *Canadian Highway Bridge Design Code,* CSA S6:19, Canadian Standards Association, Toronto, ON, Canada, 2019.

[18] *AASHTO LRFD Bridge Design Specifications,* 8th ed., American Association of State Highway and Transportation Officials, Washington, DC, USA, 2017.

[19] M.Y. Abu-Farsakh, Q. Chen, and M.N. Haque, "Calibration of resistance factors for drilled shafts for the new FHWA design method," Federal Highway Administration, FHWA/LA. 12/495, Jan. 2013, [Online]. Available: https://rosap.ntl.bts.gov/view/dot/25677.

[20] F. Naghibi and G.A. Fenton, "Target geotechnical reliability for redundant foundation systems," *Can. Geotech. J.,* vol. 54, no. 7, pp. 945–952, 2017, https://doi.org/10.1139/cgj-2016-0478.

[21] I.M. Smith, D.V. Griffiths, and L. Margetts, *Programming the finite element method,* 5th ed. New York, NY, USA: John Wiley & Sons, 2013.

[22] R. Rahimi, Y. Liu, and G.A. Fenton, "Parallelized finite element algorithms for modeling unreinforced concrete masonry infilled RC frames," *Can. J. Civ. Eng.,* vol. 8, no. 2, pp. 115–123, 2021, https://doi.org/10.1139/cjce-2020-0655.

[23] G. Esposito, G.A. Fenton, and F. Naghibi, "Seismic reliability of axially-loaded vertical piles," *Can. Geotech. J.,* vol. 57, no. 12, pp. 1805–1819, 2020, https://doi.org/10.1139/cgj-2019-0342.

[24] G. Esposito and G.A. Fenton, "Seismic reliability of deep foundations with soil-structure interaction," unpublished manuscript, to be submitted to *Can. Geotech. J.,* 2022.

[25] Natural Resources Canada, "Hazard Calculator," 2015. [Online]. Available: http://www.seismescanada.rncan.gc.ca/hazard-alea/interpolat/index-en.php.

[26] J. Humar, "Background to some of the seismic design provisions of the 2015 National Building Code of Canada," *Can. J. Civ. Eng.,* vol. 42, no. 11, pp. 940-952, 2015, doi: doi.org/10.1139/cjce-2014-0385.

[27] A. Al Mamun and M. Saatcioglu, "Analytical modeling of moderately ductile RC frame structures for seismic performance evaluation using PERFORM-3D," *Earthq. Spectra,* vol. 35, no. 2, pp. 635–652, 2019, https://doi.org/10.1193%2F081016EQS131M.

[28] *British Columbia Building Code 2018.* Buidling and Safety Standards Branch, Victoria, BC, Canada, 2018.

[29] P. He, G.A. Fenton, and D.V. Griffiths, "Calibration of resistance factors for bearing resistance design of shallow foundations under seismic and wind loading," unpublished manuscript, submitted to *Can. Geotech. J.,* 2021.

[30] K. Terzaghi, *Theoretical soil mechanics.* New York, NY, USA: John Wiley & Sons, 1943.

[31] Computers and Structures, Inc., Berkeley, CA, USA, *SAP2000,* ver. 21.0.2, 2019. [Online]. Available: https://www.csiamerica.com/products/sap2000.

[32] F. Naghibi and G.A. Fenton, "Calibration of resistance factors for geotechnical seismic design," *Can. Geotech. J.,* vol. 56, no. 8, pp. 1134–1141, 2019, https://doi.org/10.1139/cgj-2018-0433.

[33] R.G.M. de Munck. "Geotechnical seismic design code calibration: A probabilistic study of seismic design code safety," Ph.D. dissertation, Delft University of Technology, Delft, Netherlands, 2020.

[34] L. Sanpaolesi, Ed. "Scientific support activity in the field of structural stability of civil engineering works: Snow loads," Commission of the European Communities, DGIII-D3, Brussels, Belgium, Tech. Rep. Contract no. 500990, 1999.

[35] E. Simiu, A.L. Pintar, D. Duthinh, and, D. Yeo, "Wind load factors for use in the wind tunnel procedure," *ASCE-ASME J. Risk UA.,* vol. 3, no. 4, 2017, https://doi.org/10.1061/ajrua6.0000910.

[36] I.K. Lee, W. White, and O.G. Ingles. *Geotechnical Engineering.* London, UK: Pitman, 1983.

[37] G.A. Fenton, D.V. Griffiths, and O.O. Ojomo, "Consequence factors in the ultimate limit state design of shallow foundations," *Can. Geotech. J.,* vol. 48, no. 2, pp. 265–279, 2011, https://doi.org/10.1139/T10-053.

[38] *Minimum design loads and associated criteria for buildings and other structures, ASCE/SEI 7-16, American Society of Civil Engineers,* Reston, VA, USA, 2017, https://doi.org/10.1061/9780784414248.

[39] B.R. Ellingwood and P.B. Tekie, "Wind load statistics for probability-based structural design," *J. Struct. Eng.,* vol. 125, no. 4, pp. 453–463, 1999, https://doi.org/10.1061/(ASCE)0733-9445(1999)125:4(453).

[40] P. He and G.A. Fenton, "Calibration of resistance factors for design of strip foundations against sliding," unpublished manuscript, submitted to *Can. Geotech. J.,* 2022.

[41] R.M. Barker, J.M. Duncan, K.B. Rojiani, P.S. Ooi, C.K. Tan, and S.G. Kim, "Manuals for the design of bridge foundations: Shallow foundations, driven piles, retaining walls and abutments, drilled shafts, estimating tolerable movements, load factor design specifications and commentary," Washington, DC, USA, Transportation Research Board, Tech. Rep. NCHRP 343, Dec. 1991.

[42] G.A. Fenton, D.V. Griffiths, and X. Zhang, "Load and resistance factor design of shallow foundations against bearing failure," *Can. Geotech. J.,* vol. 45, no. 11, pp. 1556–1571, 2008, https://doi.org/10.1139/T08-061.

[43] A. Nour, A. Slimani, and N. Laouami, "Foundation settlement statistics via finite element analysis," *Comput. Geotech.,* vol. 29, no. 8, pp. 641–672, 2002, https://doi.org/10.1016/S0266-352X(02)00014-9.

[44] G.A. Fenton, D.V. Griffiths, and W. Cavers, "Resistance factors for settlement design," *Can. Geotech. J.,* vol. 42, no. 5, pp. 1422–1436, 2005, https://doi.org/10.1139/t05-053.

[45] P. He, G.A. Fenton, and D.V. Griffiths, "Calibration of resistance factors for gravity retaining walls," unpublished manuscript, submitted to *Can. Geotech. J.,* 2022.

[46] J.S. Kim, "Reliability-based design of a retaining wall," Ph.D. dissertation, Virginia Polytechnic Institute and State University, Blacksburg, VA, 1995.

[47] X.Z. Wu, "Trivariate analysis of soil ranking-correlated characteristics and its application to probabilistic stability assessments in geotechnical engineering problems," *Soils Found.,* vol. 53, no. 4, pp. 540–556, 2013, https://doi.org/10.1016/j.sandf.2013.06.006.

[48] S. Javankhoshdel and R.J. Bathurst, "Influence of cross correlation between soil parameters on probability of failure of simple cohesive and c-ϕ slopes," *Can. Geotech. J.,* vol. 53, no. 5, pp. 839–853, 2015, https://doi.org/10.1139/cgj-2015-0109.

[49] R.K. Rowe and J.R. Booker, "The behaviour of footings resting on a non-homogeneous soil mass with a crust. Part I. Strip footings," *Can. Geotech. J.,* vol. 18, no. 2, pp. 250–264, 1981, https://doi.org/10.1139/t81-028.

CSA Group Research

In order to encourage the use of consensus-based standards solutions to promote safety and encourage innovation, CSA Group supports and conducts research in areas that address new or emerging industries, as well as topics and issues that impact a broad base of current and potential stakeholders. The output of our research programs will support the development of future standards solutions, provide interim guidance to industries on the development and adoption of new technologies, and help to demonstrate our on-going commitment to building a better, safer, more sustainable world.

CSA GROUP™